IN THE UNITED STATES PATENT AND TRADEMARK OFFICE

In re Application of:	Mark L. Weiss		
Serial No.:	10/647,361	Group No.:	1632
Filed:	08/25/2003	Examiner:	Thaian Ton
Entitled:	**Cultures, Products and Methods Using Stem Cells**		

SECOND DECLARATION OF DR. KATHY MITCHELL

EFS WEB-FILED
Commissioner for Patents
P.O. Box 1450
Alexandria, VA 22313-1450

I, Dr. Kathy Mitchell, state as follows:

1. My present position is Senior Scientist, Message Pharmaceuticals, 1448 S. Rolling Road Baltimore, MD 21227. Message Pharmaceuticals is a licensee of the above referenced patent application.

2. I am an inventor of the above referenced patent application.

3. It is my understanding that Examiner has rejected the claims as being non-enabled, lacking an adequate written description, and as anticipated by Purchio et al., U.S. Pat. No. 5,919,702. In the telephonic interview on October 28, 2008, the Examiner suggested presenting data that further described the claimed cell population and that demonstrated how the cell population obtained by the claimed process differ from the prechondrocytes of Purchio et al. and the Wharton's Jelly extract used by Purchio et al. as well as embryonic stem cells.

4. The cell population obtained by the process described in the claims:, a) enzymatically dispersing umbilical cord matrix to provide enzymatically dispersed umbilical cord matrix cells; b) culturing the enzymatically dispersed umbilical cord matrix cells in the presence of epidermal growth factor (EGF) and platelet derived growth factor (PDGF) to proliferate the umbilical cord matrix cells; c) culturing the enzymatically dispersed umbilical cord matrix cells on a substrate surface and removing non-adherent cells; and d) culturing

adherent cells from (c) to select for a population of umbilical cord matrix cells that comprise cells that are negative for CD34 and CD45, positive for telomerase activity, can be expanded in vitro, and maintained in culture through repeated passages differs significantly from the Purchio prechondrocytes and embryonic stem cells.

5. Cells isolated from Wharton's jelly of umbilical cords by the method of Purchio et al., (Figure 1) were allowed to migrate from the tissue and expand for 10-12 days as described. The Purchio prechondrocytes were harvested by trypsinization, replated and expanded for 4 passages. Purchio et al. does not describe a cell population obtained by enzymatic dispersion of Wharton's jelly. Cells were isolated from umbilical cord matrix by the method of Weiss et al. by using enzymatic dispersion (in this case hyaluronidase and collagenase) and mechanical disruption followed by plating for expansion. The umbilical cord matrix stem cells (Weiss-UCMSC) were expanded for four passages.

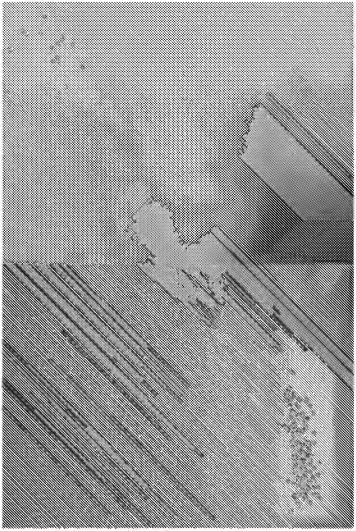

Figure 1: Cells isolated from explants of Wharton's jelly by the method of Purchio et al.,: Upper panel shows an example of cell migration from the tissue 7 days after processing. The lower panel shows an example of cells 12 days after processing of the cord just prior to harvesting by trypsinization.

6. Initial isolates of Weiss-UCMSC (P0) were analyzed for seven cell surface markers by FACS (Table 1). The results from FACS analysis of Weiss-UCMSC (P0) show a general trend of lower percentage of cells positive for the HSC marker CD34 and endothelial precursor markers CD31 and CD133 than for the mesenchymal stem cell (MSC) marker, CD90. A comparison of marker expression for Weiss-UCMSC between P0 to P4 (Table 2) shows no significant changes in the expression pattern of these markers. Exceptions to this trend are the relatively low expression of the MSC marker, CD73 (31.7%) and high expression of the HSC marker CD45

(46.6%) by Weiss-UCMSC P0. The expression of CD45 is greatly reduced in P4 Weiss-UCMSC. The expression of CD73 and CD45 are also significantly different in P4 Weiss-UCMSC (93.6% and 1.6%, respectively) reflecting a more MSC-like phenotype that is obtained after adherent cell selection and passage of the cells in culture medium containing PDGF and EGF, favoring growth of undifferentiated MSC.

Table 1: FACS Analysis of Cell Surface Marker Expression of P0 Weiss-UCMSC

	CD31	CD34	CD45	CD73	CD90	CD133	CD146
mean	0.56%	2.4%	46.6%	31.7%	94.4%	10.8%	9.3%
S.D.	0.88%	3.2%	31.8%	27.8%	6.7%	13.9%	5.6%
n	5	7	5	5	7	5	3

Table 2: FACS Analysis of Cell Surface Marker Expression of Weiss-UCMSC and Purchio Prechondrocytes.

			PURCHIO			**KSU**				
	Mean	**SD**	**SEM**	**N**	**Mean**	**SD**	**SEM**	**N**	**P**	
CD13	98.4	0.17	0.07	6	98.3	0.25	0.13	4	0.58	
CD29	98.4	0.09	0.04	6	98.5	0.1	0.06	3	0.17	
CD31	12.9	28.8	11.8	6	0.43	0.67	0.33	4	0.42	
CD34	0.63	0.60	0.25	6	0.08	0.15	0.08	4	0.11	
CD44	95.4	1.4	0.56	6	97.7	0.92	0.46	4	0.02	**
CD45	8.1	15.0	6.2	6	1.6	0.43	0.21	4	0.47	
CD73	94.2	3.9	1.6	6	93.6	7.2	3.6	4	0.86	
CD90	98.5	0.06	0.03	6	98.4	0.22	0.11	4	0.22	
CD105	76.2	12.8	5.2	6	89.7	1.9	0.96	4	0.075	*
CD133	1.4	1.2	0.49	6	2.7	0.65	0.33	4	0.0879	*
CD146	61.5	16.0	6.5	6	16.9	6.5	3.3	4	0.0008	***

Unpaired T-test results of data from FACS analysis of P4 cells Weiss-UCMSC and Purchio Prechondrocytes. * $p<0.10$, ** $p<0.05$, *** $p<0.01$

7. The data in paragraph 5 demonstrates that the cell population obtained by the process of enzymatic dispersion and adherent cell selection is substantially different from the cell population produced by Purchio's methods. This difference is demonstrated by the differences in cell surface markers. The cell population obtained following the processing steps is a substantially different cell population.

8. There are also other differences between unprocessed Wharton's jelly and the cell population obtained by the claimed processing steps. The Wharton's jelly in Purchio et al. is described as follows:

> Wharton's jelly is a gelatinous substance found in the umbilical cord which has been generally regarded as a loose mucous connective tissue, and has been frequently described as consisting of fibroblasts, collagen fibers and an amorphous ground substance composed mainly of hyaluronic acid (Takechi et al., 1993, Placenta 14:235-45). Various studies have been carried out on the composition and organization of Wharton's jelly (Gill and Jarjoura, 1993, J. Rep. Med. 38:611-614; Meyer et al., 1983, Biochim. Biophys. Acta 755:376-387). One report described the isolation and in vitro culture of "fibroblast-like" cells from Wharton's jelly (McElreavey et al., 1991, Biochem. Soc. Trans. 636th Meeting Dublin 19:29S).

Lacking in the description provided by Purchio et al., is a description of the structural features of the entirety of the umbilical cord, of which Wharton's jelly is only part, and a full description of the complex structure of Wharton's jelly itself. The fully developed umbilical cord has one vein and two arteries surrounded by mucous or gelatinous connective tissue, the Wharton's jelly component, all of which is covered with amnion (Fig. 1). There are three distinct zones of stromal cells and matrix that can be identified in the umbilical cord: the subamniotic layer, Wharton's jelly, and the media and adventitia surrounding the vessels (Mitchell 2005 and references therein). The Wharton's jelly region is the most abundant and has cleft-like spaces of stromal matrix molecules of collagens type I, III, and VI, with collagen type VI, laminin, and heparin sulphate proteoglycan around the clefts. The jelly-filled, cleft-like spaces are surrounded by stromal cells that are slender and spindle shaped myofibroblasts which express vimentin and smooth muscle actin as well as desmin (Mitchell 2005).

We have investigated the localization of proteins expressed by umbilical cord matrix cells *in situ* and found that they are expressed by cells in specific regions of the umbilical cord. Oct-4 is a transcription factor primarily expressed by undifferentiated pluripotent stem cells and vimentin is an intermediate filament expressed by primitive myofibroblasts, mesenchymal stem cells (MSC) and other types of precursor cells. Figure 2 demonstrates that the Oct-4 and vimentin-expressing cells in the umbilical cord are confined to specific regions, near the vessels and beneath the amnion. This perivascular localization of the cells expressing stem cell markers is typical of the

localization of MSC in adult tissues and organs. Note that the major portion of Wharton's jelly is *not* populated by cells which express these markers as shown in Figure 2. However, this region is not acellular based on histochemical staining (data not shown). Thus, UCMS cells can be isolated from only a fraction of the entire umbilical cord matrix regions. ***Stripping the amniotic covering or vessels, as described by the method of Purchio et al., without extreme care would essentially eliminate these stem cells from the Wharton's jelly prior to its culturing.***

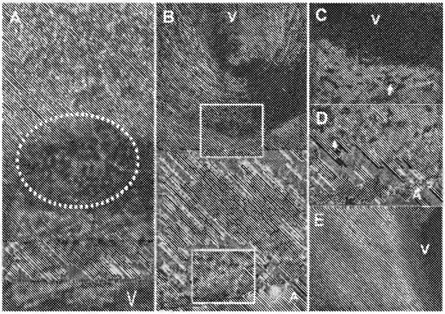

Figure 2: Oct-4 and vimentin-expressing cells in umbilical cord cross sections: **A)** Cross sections (10 µm) of umbilical cord were probed for Oct-4 expression with DAB as a chromogen. Immunoreactivity (dark brown staining was observed in the rounded central portions of cells that are found in clusters (circled) near the vessels (V) and amnion (A). **B)** A composite image of a human umbilical cord shows vimentin-positive cells near the vessels (V) and beneath the amnion (A). Magnification of boxed regions in Panel B show vimentin positive cells (arrows) near the vessels (**C**) and beneath the amnion (**D**). Panel E shows a typical example of an umbilical cord cross section probed with secondary antibody alone. Note the absence of vimentin and/or Oct-4 positive cells in the major portion of the Wharton's jelly between the vessels and the amnion.

In summary:

- From the perspective of the complex structure of the matrix and how the cells are "entrapped" in lacunae surrounded by matrix consisting of collagen and proteoglycans, it

seems obvious that enzymatic digestion of those specific molecules by collagenase and hyaluronidase would be required to free to them.

- Only migratory cells can be isolated from the explants by method of Purchio.
- FACS analysis of cells of the invention of Weiss et al., are 100% vimentin positive (data not shown). Vimentin- positive cells are only found in specific regions of the cord matrix which is lost by the method of Purchio wherein the amnion and vessels are stripped and only the component of umbilical cord matrix consisting of Wharton's jelly is cultured.

9. The data in paragraph 6 demonstrates that the cell population obtained by the process of enzymatic dispersion and adherent cell selection is substantially different from the cell population obtained by the method of Purchio et al. In Purchio et al., the Wharton's jelly is cultured as follows:

> Wharton's jelly is collected from the umbilical cord under sterile conditions by any appropriate method known in the art. For example, the cord is cut transversely with a scalpel, for example, into approximately one inch sections, and each section transferred to a sterile container, such as a 50 ml centrifuge tube, containing a sufficient volume of phosphate buffered saline (PBS) containing $CaCl_2$ (0.1 g/l) and $MgCl_2 6 H_2O$ (0.1 g/l) to allow surface blood to be removed from the section upon gentle agitation. The section is then removed to a sterile-surface where the outer layer or "casing" of the section is sliced open along the cord's longitudinal axis. Wharton's jelly is typically located between the three blood vessels of the umbilical cord. The blood vessels and casing are dissected away, for example, with sterile forceps and dissection scissors, and the Wharton's jelly is collected and placed in a sterile container, such as a 100 mm TC-treated Petri dish. The Wharton's jelly may then be cut into smaller sections, such as 2-3 mm^3, for culturing.

Purchio, Column 11, lines 8-25. Thus, in Purchio et al., a section of Wharton's jelly is removed from the umbilical cord and cultured. As shown in Table 2, this process results in a substantially different cell population than is produced by the claimed method. In total, the percentage of cells expressing of four of the eleven cell markers is significantly different between the two populations. Purchio prechondrocytes and Weiss-UCMSC were analyzed by FACS at P4 for eleven cell surface markers (Table 2). The matrix receptors, CD44 and CD105, both important for differentiation of MSC, are expressed at significantly higher levels in Weiss-

UCMSC than in Purchio prechondrocytes. In addition, CD133, an endothelial precursor marker that is observed in some MSCs, is expressed at higher levels in Weiss-UCMSC although overall expression is still low (2.7%). CD146, a pericyte marker that has recently been identified in many tissue-specific MSC, is expressed at higher levels in Purchio prechondrocytes than in Weiss-UCMSC (61.5% vs 16.9%, respectively).

10. There is a striking difference in morphology of the cells obtained by the method of Purchio et al., and Weiss et al., in high density cultures although the cellular morphology is similar at low density (Figures 3, 4). In addition to differences in the cellular morphology between Weiss-UCMSC which are rounded spindle-shaped cells compared to the thin, elongated shape observed for the majority of Purchio prechondrocytes at high density, the overall appearance and organization of the cells is also very different (Figure 3, 4). The Weiss-UCMSC form embryoid body-like structures when approaching confluence (Figure 2). Similar structures have not been observed in cultures of Purchio prechondrocytes which become aligned and tightly packed with some regions showing an interwoven appearance (Figure 4).

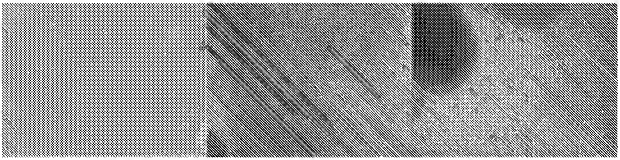

Figure 3: Weiss-UCMSC P4 at left) low density, center) higher density and right) overconfluence. Note the spindle-shaped myofibroblast-like morphology of the UCMSC and the formation of embryoid body-like colonies at higher culture densities.

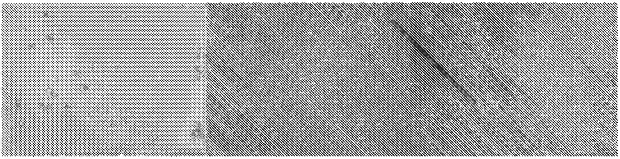

Figure 4: Purchio P4 prechondrocytes at left) low density, center) higher density and right) overconfluence. Note the spindle-shaped myofibroblast-like morphology of the prechondrocytes that is similar to UCMSC at low density. In contrast the high density cultures show cells with strikingly different morphology than UCMSC high density cultures. Most notable is the absence of embryoid body-like colonies and the "woven" highly organized appearance of the high density prechondrocyte cultures.

11. There is also a substantial difference in the ability of the Purchio cells to differentiate as opposed to the Weiss-UCMSC. To determine if the Purchio prechondrocytes are multipotential and can differentiate across cell lineages, they were treated with a neuronal induction protocol shown to induce neuronal differentiation of Weiss-UCMSC. Both Purchio prechondrocytes and Weiss-UCMSC were also treated with adipocyte, chondrogenic and osteogenic induction medium to show mesodermal lineage potential. Purchio prechondrocytes were not capable of neuronal differentiation when treated by the method of Woodbury et al., (2000) which was demonstrated to differentiate Weiss-UCMSC into neuronal pheuotypes (Mitchell et al., 2003). Figure 5 shows the Purchio prechondrocytes and Weiss-UCMSC treated with neuronal induction Adipogenic, chondrogenic and osteogenic differentiation of Weiss-UCMSC and Purchio prechoondrocytes are shown in Figure 6. Both Weiss-UCMSC and Purchio prechondrocytes can differentiate into mesodermal lineage cells, while only Weiss-UCMSC can differentiate into neuronal cells of ectodermal lineage. This suggests that Weiss WJC are pluripotent while Purchio prechondrocytes clearly are not.

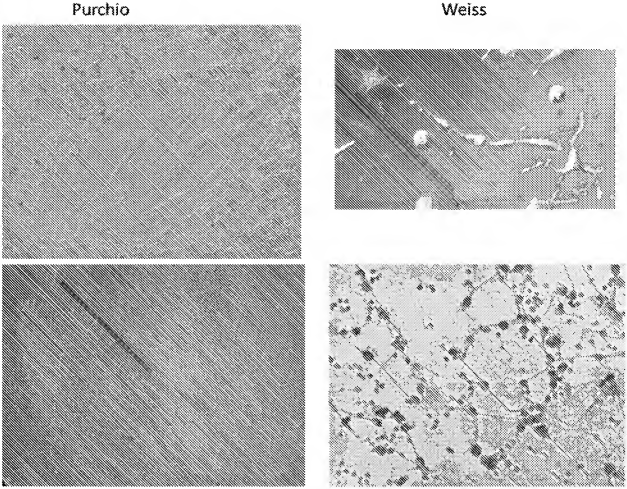

Figure 5: Neuronal induction of Purchio prechondrocytes and Weiss-UCMSC. Purchio prechondrocytes do not display a neuronal morphology (left panels) as is observed for the neuronally induced Weiss-UCMSC (right panels) which show dendrite and axon-like processes and the formation of primitive networks reminiscent of cultures of primary neurons. In contrast the Purchio prechondrocytes display a morphology that is unchanged from the cells grown in the Purchio expansion medium (Figure 4).

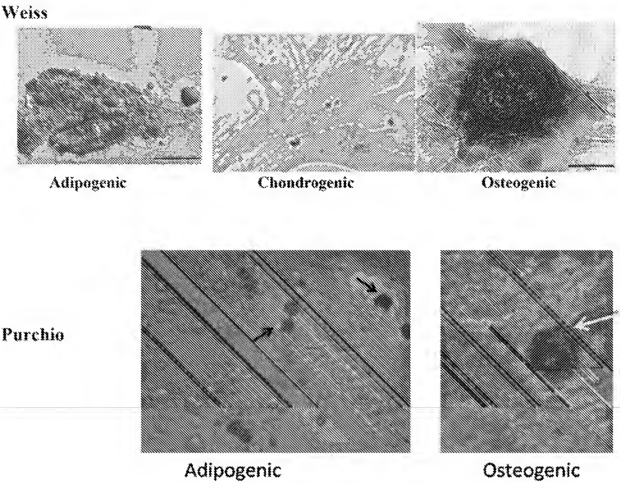

Figure 6: Adipogenic, chondrogenic and osteogenic differentiation of Weiss-UCMSC and adipogenic and osteogenic Purchio prechoondrocytes (arrows indicate lipid droplet containing round adipocyte-like cells in the Purchio adipogenic differentiation and mineralization in the osteogenic differentiation medium).

12. The data presented in paragraph 5 further demonstrate that populations of cells isolated by the claimed process steps are clearly distinguishable for embryonic stem cells. In particular, cell populations made by the claimed process steps have different cell surface markers than embryonic stem cells.

14. I further declare that all statement made herein of my own knowledge are true and that all statements made on information and belief are believed to be true; and further that these

statements were made with the knowledge that willful false statements and the like so made are punishable by fine or imprisonment, or both, under section 1001 of title 18 of the United States Code, and that such willful false statements may jeopardize the validity of the application or any patent issued thereon.

15. The following references are attached:

Tab 1. Hirko, A., R. Dallasen, S. Jomura, Y. Xu (2008) Modulation of inflammatory responses after global ischemia by transplanted umbilical cord matrix stem cells. Stem Cells Express, published online August 21, 2008; doi:10.1634/stemcells

Tab 2. Jomura, S., C. Bode, M. Uy, K.E. Mitchell, R. Dallasen, Y. Xu. (2007) Potential treatment of cerebral global ischemia with Oct-4+ umbilical cord matrix stem cells. *Stem Cells*, 25 (1), 98-106.

Tab 3. Mitchell, K.E. (2005) "Umbilical Cord Stem Cells", Stem Cells in Endocrinology, Humana Press, Editor, Linda Lester, pp 49-66

Dated: November 2, 2009

Kathy E Mitchell

Dr. Kathy Mitchell

TAB 1

Stem Cells Express, published online August 21, 2008; doi:10.1634/stemcells.2008-0075

STEM CELLS®

TISSUE-SPECIFIC STEM CELLS

Modulation of Inflammatory Responses after Global Ischemia by Transplanted Umbilical-Cord Matrix Stem Cells

Aaron Hirko[1], Renee Dallasen[1], Sachiko Jomura,[1,&] Yan Xu[1,2,3,*]

Departments of [1]Anesthesiology, [2]Pharmacology, and [3]Structural Biology, University of Pittsburgh School of Medicine, Pittsburgh, PA 15260

Key words. Umbilical cord matrix stem cells • Stroke • Reactive astrocytosis • Microglia • Vimentin • Nestin • Stem cells

ABSTRACT

Rat umbilical cord matrix (RUCM) cells are stem-cell-like cells and have been shown to reduce neuronal loss in the selectively vulnerable brain regions after cardiac arrest (CA). Here, we investigate whether this protection is mediated by the RUCM cells' modulation of the post-ischemia inflammation responses, which have long been implicated as a secondary mechanism of injury following ischemia. Brain sections were examined immunohistochemically for GFAP, vimentin, and nestin as markers for astroglia and reactive astrogliosis, Ricinus Communis Agglutinin-1 (RCA-1) as a marker for microglia, and Ki67 as a marker for cell proliferation. Rats were randomly assigned to six experimental groups: (1) 8-min CA without treatment, (2) 8-min CA pretreated with culture medium injection, (3) 8-min CA pretreated with RUCM cells, (4) sham-operated CA, (5) medium injection without CA, and (6) RUCM cell transplantation without CA. Groups 1-3 have significantly higher Ki67$^+$ cell counts and higher GFAP$^+$ immunoreactivity in the hippocampal CA1 region compared to groups 4-6, irrespective of treatment. Groups 1 and 2 have highly elevated GFAP$^+$, vimentin$^+$, and nestin$^+$ immunoreactivity, indicating reactive astrogliosis. Strikingly, RUCM cell treatment nearly completely inhibited the appearance of vimentin$^+$ and greatly reduced nestin$^+$ reactive astrocytes. RUCM cell treatment also greatly reduced RCA-1 expression, which is found to strongly correlate with the neuronal loss in the CA1 region. Our study indicates that treatment with stem-cell-like RUCM cells modulates the inflammatory response to global ischemia and renders neuronal protection by preventing permanent damage to the selectively vulnerable astrocytes in the CA1 region.

INTRODUCTION

Cerebral global ischemia secondary to cardiac arrest (CA) causes oxygen and glucose deprivation in the brain, leading to brain damage or death unless cerebral blood flow is restored immediately. Ischemic brain injury is characterized by a delayed selective loss of vulnerable CA1 pyramidal neurons in the hippocampus. Post ischemic inflammatory response is thought to be a major contributor to the delayed neuronal loss following ischemia [1, 2] and involves both reactive astrocytosis and microgliosis in and around the damaged area of the brain [3, 4].

The process of reactive astrocytosis consists of hyperplasia and hypertrophy of astrocytes along

Author contributions: A.H.: Data collection, analysis, and interpretation; manuscript/figure preparation. R.D.: Data collection; tissue preparation for histology; stem cell culturing; S.J.: Data collection; cardiac arrest and resuscitation; stem cell culturing; Y.X.: Conception and design, financial support, provision of study material; data interpretation; manuscript writing, final approval of manuscript

* Address all correspondence to: Professor Yan Xu, University of Pittsburgh School of Medicine, 2048 Biomedical Science Tower 3, 3501 Fifth Avenue, Pittsburgh, PA 15260, (412) 648-9922, Fax (412) 648-8998; (&Current address: Kansai Medical University, Department of Anesthesiology, 2-3-1 Shinmachi Hirakata City, Osaka, Japan 573-1191); Received January 24, 2008; accepted for publication August 05, 2008; first published online in Stem Cells Express August 21, 2008. ©AlphaMed Press 1066-5099/2008/$30.00/0 doi: 10.1634/stemcells.2008-0075

with the concomitant up-regulation of intermediate filaments such as glial fibrillary acidic protein (GFAP), vimentin (VIM), and the re-expression of nestin (NES) [5]. Acutely reactive astrocytosis appears to be neuroprotective [6]. At later time points, however, the reactive astrocytosis and the resulting glial scarring have been shown to cause a physical and biochemical barrier to axonal regeneration and synaptogenesis, hindering neuronal repair and recovery [7].

The process of microgliosis involves the activation of resident microglia along with the recruitment of peripheral macrophages in and around the ischemia-damaged areas where these cells serve as scavengers for clearing the cellular debris. They can also secrete a variety of cytotoxic and protective chemicals [8]. A number of studies, with treatment strategies aimed at reducing microglial activation, have shown to reduce neuronal damages after the treatment [9-12]. On the contrary, others have shown that microglia may actually play a protective role after ischemia [13-15].

We have recently demonstrated that transplantation of rat umbilical-cord matrix (RUCM) cells can provide partial protection against neuronal injury after global ischemia [16]. These cells, derived from the Wharton's jelly of the umbilical cord, are primitive stem-cell-like cells [17]. They are positive for several important stem cell markers, particularly Oct-4, can be expanded far beyond the Hayflick limit in culture, and can be induced to differentiate into several cell types [17, 18]. Rats treated with RUCM cells three days prior to an 8-min CA had only 25-32% neuronal loss in the hippocampal CA1 region compared to the typical 50-68% neuronal loss observed in the untreated or the vehicle-treated animals. Transdifferentiation and stem cell fusion with the host cells were ruled out as the predominating mechanisms for the protection. Other mechanisms, including extracellular signaling, were suggested. Given the fact that inflammatory responses may play a defining role in the delayed neuronal damage, this study aims at examining the mitigating effects of the stem-cell-like RUCM cells on the post-ischemia inflammatory response as a possible mechanism of neuroprotection.

Material And Methods

Animal Groups

All animal protocols were approved by the Institutional Animal Care and Use Committee of the University of Pittsburgh. Paraffin-embedded brain tissues, randomly selected from four experimental groups in the previously reported studies [16] and two additional groups added for this investigation, were combined and examined. The six experimental groups are: (1) 8-min cardiac arrest alone (CA only, n = 6); (2) microinjection of the defined media (DM) at four unilateral locations, as detailed previously [16], followed three days later by an 8-min cardiac arrest (DM + CA, n = 7); (3) transplantation of stem-cell-like RUCM cells at the same four unilateral locations followed three days later by an 8-min cardiac arrest (RUCM + CA, n = 6); (4) sham-operated cardiac arrest without pretreatment (sham, n = 4), (5) microinjection of defined media unilaterally at the same four locations without cardiac arrest (DM only, n = 4), and (6) transplantation of RUCM unilaterally at the same four locations without cardiac arrest (RUCM only, n = 5). The DM is composed of the Dulbecco modified Eagle's medium (Invitrogen, Carlsbad, CA) and MCDB-201 medium (Sigma-Aldrich, St. Louis, MO) supplemented with 1x insulin-transferrin-selenium (Invitrogen), 2% fetal bovine serum (BD Biosciences, San Jose, CA), 0.1 nM dexamethasone (Sigma-Aldrich), 0.15% lipid-rich bovine serum albumin (Albumax from Invitrogen), 10 µM ascorbic acid-2-phosphate (Sigma-Aldrich), 1x penicillin/streptomycin (Thermo-Fisher, Suwanee, GA).

Cardiac Arrest and Resuscitation

CA and resuscitation were performed as described before [16, 19-22]. Briefly, male Sprague-Dawley rats weighing 234 ± 27 g (Harlan Sprague Dawley, Inc., Indianapolis, IN)

were subjected to a clinically relevant outcome model of CA. Under isoflurane anesthesia, rats were intubated orotracheally, mechanically ventilated, and paralyzed with pancuronium bromide (2 mg/kg). CA was induced by an i.v. bolus injection of an ultra-short-acting β_1-blocker, esmolol (6.25 mg), along with the stoppage of mechanical ventilation. Resuscitation was started either immediately (sham) or after 8 minutes by 100% O_2 ventilation along with a retrograde infusion of oxygenated blood mixed with resuscitation mixture containing heparin (5 U/ml), sodium bicarbonate (0.05 mEq/ml), and epinephrine (8 µg/ml).

RUCM cell transplantation

As characterized in detail previously [16], RUCM cells were cultured and confirmed to be Oct-4 positive. Multiple lines of experimental evidence, including immunohistochemistry, flow cytometry, transcript analysis, and karotype stability beyond Hayflick limit, support the notion that these cells are stem-cell-like cells (meaning that they show some characteristics of stem cells). Three days prior to CA, approximately 4 × 10 [4] RUCM cells in 10 µL (2.5 µL at each site) were injected at the following four sites in the left hemisphere: dorsal thalamic nucleus, dorsal hippocampus, corpus callosum (CC), and dorsal cortex. As controls, defined medium was injected in the exact same manner at the same four locations.

Tissue Preparation

Ten days after RUCM cell or DM injection and seven days after CA and resuscitation, rats were anesthetized with isoflurane and perfused with buffered 10% formalin phosphate. The brain was extracted from the skull and stored in buffered 10% formalin for 48 hours. The brain section containing the dorsal hippocampal region was embedded in paraffin and sliced into 6-µm-thick coronal sections using an American Optical model 820 microtome. Approximently 40 sections were collected from the region between −3.5 and −3.75 mm from the bregma. Two sections spaced apart by a section were randomly selected for each type of staining. Another two sections, approximately 15 sections posterior to the first two, were also selected for each staining.

Immunostaining

Sections were deparaffinized, rehydrated, and then boiled in 10 mM sodium citrate (pH = 6.0) for antigen retrieval. Standard immunohistochemistry techniques were used. The primary antibodies were incubated overnight at 4°C using mouse anti-GFAP (1:200) from Neuromics (Edina, MN); rabbit anti-vimentin (1:200), rabbit anti-Ki67 (1:100), and goat anti-Iba1 (1:50) from Abcam (Cambridge, MA); and biotinylated RCA-1 (1:2000) from Vector Laboratories (Burlingame, CA). Secondary antibodies used in the study were Alexa Fluor 594 goat anti-mouse IgG_{2a} (1:500), Alexa Fluor 488 goat anti-mouse IgG_1 (1:500), and Alexa Fluor 488 goat anti-rabbit IgG (1:500) from Invitrogen; Cy3 goat anti-rabbit (1:250) from Jackson Immunoresearch (West Grove, PA); and biotinylated goat anti-rabbit (1:500) from Dako (Glostrup, Denmark). For diaminobenzidine (DAB) staining, sections were incubated with ExtrAvidin peroxidase (HRP) conjugate (1:1,000; Sigma-Aldrich). Tissues labeled with HRP were developed with a solution of 0.67 mg/ml DAB (Sigma-Aldrich) and 0.13 µl of 30% H_2O_2 per mL of PBS [23]. DAB-stained slides were then dehydrated and cleared in xylene and coverslipped with Eukitt mounting medium (EMS, Hatfield, PA). For fluorescence imaging, nuclear DNA was stained with 4'-6-diamidino-2-phenylindole (DAPI) 1 µg/mL in PBS (Sigma-Aldrich) and coverslipped using Fluoromount-G (Southern Biotech, Birmingham, AL).

Images were acquired using the In Vivo 3.2 software (Media Cybernetics, Bethesda, MD) driving an Olympus IX81 microscope (Tokyo, Japan) with a Prior motorized stage, a Sutter Lambda xenon exciter light source, an Olympus disc-scanning unit (DSU), and captured with an ORCA-ER (Hamamatsu, Japan) digital camera. All images were post-processed and analyzed in

a blinded manner (i.e., investigators were unaware of the group identities) using Image-Pro AMS (Media Cybernetics). Percent positive area stained for GFAP, NES, and RCA-1 in the CA1 regions were analyzed by thresholding segmentation. The CA1 regions of interest were defined by closely outlining the cell layer as determined by using the DAPI nuclear staining (see online supplementary materials). The same regions used for determining the percent positive areas were used for cell counts. GFAP$^+$ cell density was also calculated by counting all GFAP$^+$ cell soma (defined as an area of GFAP$^+$ immunoreactivity clearly in association with a nuclear stain, see online supplementary materials) in the image plane of the CA1 pyramidal cell layer, normalized by the area within which the counting was performed. Vimentin was analyzed by counting VIM$^+$ cells within the CA1 region of the hippocampus. Ki67 was analyzed by counting Ki67$^+$ cells in four pre-determined, non-overlapping, equally spaced, 0.15 mm^2 circles on each side of the hippocampus.

Data Analysis

Statistical analysis was performed using SigmaStat software (Systat Software, Inc, San Jose, CA) and GraphPad PRISM (GraphPad Software, Inc., San Diego, CA). Three-way ANOVA was performed using brain side (injected and contralateral), cardiac arrest (with and without), and treatment type (none, DM, or RUCM) as group identifiers (categorical factors). When a significant result was detected with ANOVA, a post hoc Holm-Sidak test was used for pair-wise comparisons. The results are reported as mean ± SEM, and a p value of < 0.05 was considered significant.

RESULTS

Glial fibrillary acidic protein immunostaining

Upregulation of the type 3 intermediate filament protein GFAP along with hyperplasia and hypertrophy of astrocytes are the hallmarks of astrocytosis in response to insults on the central nervous system [24]. Fluorescent immunostaining for GFAP was used to examine if pretreatment with stem-cell-like RUCM cells had any effect on astrocytosis in response to an 8-min cardiac arrest. Immunostaining revealed a significant increase in GFAP staining in the CA1 region of the hippocampus for all animals subjected to 8 min of cardiac arrest (Figure 1). At higher magnification, this increase appeared to be due to an increase both in the number of astrocytes and in the thickness as well as the number of GFAP$^+$ processes, commonly seen with reactive astrogliosis (Figure 2). Semi-quantitative analysis of the percent GFAP$^+$ area and semi-quantitative cell counting in the CA1 region supported our initial observation, revealing that the contralateral and ipsilateral (injection) sides of the CA1 regions had, respectively, 17.9 ± 3.8 % and 18.3 ± 3.5 %, and 328 ± 33 and 323 ± 24 cells/mm^2 for Group 1 (CA only); 15.2 ± 1.5 % and 15.8 ± 1.6 %, and 287 ± 10 and 317 ± 19 cells/mm^2 for Group 2 (DM + CA); 12.0 ± 3.2 % and 13.1 ± 2.3 %, and 348 ± 35 and 329 ± 41 cells/mm^2 for Group 3 (RUCM + CA); 1.8 ± 0.4 % and 1.7 ± 0.4 %, and 163 ± 10 and 147 ± 13 cells/mm^2 for Group 4 (sham); 3.4 ± 0.4 % and 4.1 ± 0.8 %, 147 ± 17 and 147 ± 15 cells/mm^2 for Group 5 (DM only); and 4.3 ± 0.6 % and 4.5 ± 1.1 %, and 186 ± 22 and 192 ± 34 cells/mm^2 for Group 6 (RUCM only). On average, the percent GFAP$^+$ areas are about 3-4 times higher in the CA groups than in the non-CA groups, whereas the GFAP$^+$ cell densities increased only by a factor of ~2 in the CA groups compared to the non-CA groups (Figure 1). This suggests that the additional percentage increases in the positive GFAP staining areas are due to thicker and more numerous astrocytic processes.

Vimentin immunostaining

Vimentin is another type 3 intermediate filament protein that is usually upregulated during reactive astrocytosis [24]. Vimentin is also expressed in radial glia and neural precursor cells. In our study, animals not subjected to cardiac arrest (Groups 4-6) appear to have little VIM staining; the trace amount appears to be associated with the injection needle tract in the

CA1 region on the injection side. Three-way ANOVA showed that cardiac arrest ($P < 0.001$), and different injection treatments (no injection, DM injection, and RUCM cell transplantation; $P = 0.002$) as categorical factors were significant sources of variation. Brain side was found not to be a significant source of variation ($P = 0.683$). A significant interaction between cardiac arrest and injection treatment was detected ($P = 0.001$). Holm-Sidak post hoc comparisons revealed that among the animals subjected to 8-min CA, Group 1 (CA only) was significantly different from Group 3 (RUCM + CA) ($P < 0.05$), and Group 2 (DM + CA) was also significantly different from Group 3 ($P < 0.001$). No differences were detected between Groups 1 and 2, or among Groups 4 (Sham), 5 (DM only), and 6 (RUCM only). In Group 1 (CA only), the VIM^+ cell counts are 90 ± 15 and 94 ± 17 per CA1 section on the injection side and contralateral side, respectively. In Group 2 (DM + CA), the range of VIM^+ cell counts is not significantly different from Group 1, being 126 ± 28 and 107 ± 34 on the injection side and contralateral side, respectively. While the total number of VIM^+ cells is significantly less than the number $GFAP^+$ cells in the same CA1 area, all VIM^+ cells in the CA1 region seem to always co-localize with $GFAP^+$ cells (Figure 1). The most striking and interesting finding is that the animals in Group 3, which received stem-cell-like RUCM cell transplantation 3 days before cardiac arrest, show a greatly reduced amount of VIM^+ cells in the hippocampal CA1 regions. On the injection side, CA1 VIM^+ cell counts for Group 3 ranged from 7 to 62 (23 ± 8). Most of these cells appeared to associate with the damage along the needle tract. On the contralateral side, two animals in Group 3 has no detectable VIM^+ cells in the CA1 region, three had counts ranging from 2 to 6, and only one animal had a count of 13 ± 10 on the different sections analyzed. All VIM^+ cells had the typical star shape associated with astrocytes (data not shown).

Nestin immunostaining

Nestin is a type 4 intermediate filament that is usually expressed in neural precursors and can also be reactivated in the reactive astrocytes. We observed from our immunostaining that Group 1 (CA only) and Group 2 (DM + CA) had high levels of NES^+ immunoreactivity on both the contralateral (Figure 3) and the injection sides in the hippocampal CA1 regions. Again, cardiac arrest and injection treatment as categorical factors were found to be a significant sources of variation ($P < 0.001$, and $P = 0.012$ respectively). A significant interaction between CA and injection treatment was detected ($P < 0.01$). Brain side was not a source of significant variation ($P = 0.93$). Post hoc analysis revealed significant differences between Groups 2 (DM + CA) and 3 (RUCM + CA) ($P = 0.003$). The percentage of positive NES staining area in the CA1 region in Group 1 (CA only) is 3.8 ± 1.0 % and 4.4 ± 1.1 % on the contralateral and injection side, respectively, and 6.7 ± 2.11 % and 7.1 ± 1.8 %, respectively, in Group 2 (DM + CA). In Group 3 with RUCM cell treatment, animals had significantly less NES^+ immunoreactivity (2.1 ± 0.8 % on the contralateral side and 1.5 ± 0.7 % on the injection side). The NES^+ cells have the typical star-like morphology (data not shown).

Microglia Response in the CA1

Microglia are the key regulators of the inflammatory response in the central nervous system. In response to insults and injuries, microglia become activated and change their morphology and function from a resting ramified state to an activated phagocytic state. We used a lectin stain (Ricinus Communis Agglutinin 1, RCA-1) to visualize the microglia response in the CA1 region of the hippocampus in our study. The animals not subjected to 8-min cardiac arrest (Groups 4-6) were virtually devoid of $RCA\text{-}1^+$ staining (Figure 4). Group 1 (CA only) and Group 2 (DM + CA) had numerous $RCA\text{-}1^+$ cells dispersed throughout the CA1 regions with the morphology of the activated, phagocytic type. Subjecting the animals to 8-min CA was a significant source of variation ($P < 0.001$), so were the different injection treatments ($P < 0.001$). Brain side was again not a significant source of variation ($P = 0.883$). The interaction between the injection treatment and CA was

highly significant ($P < 0.001$). Semi-quantitative analysis revealed that Group 1 had 17.8 ± 0.9 % and 16.0 ± 1.2 % RCA-1$^+$ areas for the injection and contralateral CA1 regions, respectively. Group 2 had 14.0 ± 2.1 % and 16.1 ± 1.8 % RCA-1$^+$ areas, respectively. Group 3 appeared to have less RCA-1$^+$ immunoactivity that was distributed in tight clusters in the CA1 region (7.1 ± 2.0 % and 6.1 ± 1.5 % RCA-1$^+$ areas in the injection and contralateral CA1 regions, respectively) and are significantly different from both Groups 1 and 2 ($P < 0.001$, Holm-Sidak post hoc test between Groups 1 and 3 or Groups 2 and 3). Direct counting of microglia proves to be difficult because even at high magnifications it is nearly impossible to determine where one cell ends and another begins especially where they form compound granular corpuscles.

Cell Proliferation

Proliferation of microglia and astrocytes is another hallmark of the inflammatory response to ischemia in the brain. Ki67 is a nuclear protein found in cells that are in all phases of the active cell cycle. We used Ki67 immunohistochemistry to examine if stem-cell-like RUCM cell treatment has a measurable effect on the increase in cell proliferation associated with the inflammatory response to ischemia. We observed an increase in the number of Ki67$^+$ cells in the CA1 region for all 8-min CA groups (Figure 5). Having or not having a cardiac arrest was found to be the major source of variation ($P < 0.001$). There were no other significant sources of variation or interactions detected..

To determine what cell types were involved in proliferation, we performed double immunolabeling studies for Ki67 along with GFAP or the microglia marker Iba-1 in Group 2 (DM + CA) and Group 3 (RUCM + CA). High-magnification DSU confocal microscopy revealed that both microglia (Figure 6A) and astrocytes (Figure 6B) were involved in the proliferation. Semi-quantitative analysis showed no significant differences between Groups 2 and 3 for the proportions of Ki67$^+$ cells that were microglia or astrocytes (data not shown).

DISCUSSION

Our study used a pretreatment strategy to examine possible mechanisms of RUCM cell-mediated neuronal protection against global cerebral ischemia, allowing us to test the hypothesis that the transplanted cells can become activated by acute ischemia and improve the global histological outcome without evoking transdifferentiation or cell fusion as the predominant modes of protection. Although posttreatment is currently the most desirable modality in many clinical situations, pretreatment strategies are also highly clinically relevant, especially considering the rapid advancement in early diagnosis and preventative medicine and the development of state-of-the-art surgical interventions. For example, in a number of advanced surgical procedures, such as implantation of automatic internal defibrillators, pediatric surgeries for repairing complex congenital malformations [25], adult cardiac surgeries involving the aortic arch [26, 27], and neurosurgeries for the repair of intracranial aneurysms [23, 28], controlled circulatory arrests resulting in cerebral global ischemia are often necessary. Developing pretreatment strategies aimed at reducing neurological complications is essential for the future advancement of these and other novel medical procedures.

The 8-min global cerebral ischemia performed in this experiment resulted in a 51.7 ± 8.7% (injection side) and 50.2 ± 7.8 % (contralateral side) loss of CA1 neurons in Group 1 (CA only), and a 70.4 ± 6.9% (injection side) and 62.1 ± 8.2 % (contralateral side) loss of CA1 neurons in Group 2 (DM + CA) [16]. Pretreatment with stem-cell-like RUCM cells (Group 3) led to significant protection, cutting neuronal loss by at least 50% to 33.8 ± 2.7 % (injection side) and 24.3 ± 4.2 % (contralateral side).

Examination of the brain tissues revealed similar results for the degree of GFAP$^+$ reactive

astrocytes and the amount of cell proliferation (as determined by Ki67 staining) for all 8-min CA groups (Groups 1-3). Although the neuronal loss from the global cerebral ischemia is not completely prevented, our study indicates that treatment with stem-cell-like RUCM cells greatly reduces the appearance of the activated microglia and the VIM^+/NES^+ reactive astrocytes in the hippocampal CA1 region in these rats. These reductions are strongly correlated with the reduction of neuronal loss in the same region. As shown in Figure 7, both VIM^+ cell counts and percent $RCA\text{-}1^+$ area are correlated with the percentage of damaged pyramidal neurons in the CA1 region, with correlation coefficients of 0.93 and 0.87, respectively.

Previous reports have shown that increases in GFAP correlates well with neuronal death following injury [29, 30]. More recent studies have suggested the possibility that the increases in $GFAP^+$ astrocytic hypertrophy might be an astroglia reaction to ischemia and can actually have neuroprotective functions [31-33]. Astrocytes can play a number of protective roles after ischemia, including the uptake and transport of glutamate and glucose, repair of the blood brain barrier, and the production and release of neurotrophic factors [34, 35]. Several studies demonstrating protection against ischemia-induced injuries by compounds targeting the inflammatory response to ischemia also show increases in GFAP immunostaining along with reductions in neuronal damage and microglia activation [11, 12, 36, 37]. We observed similar GFAP immunoreactivity increases associated with the 8-min cardiac arrest. A lack of the concomitant increases in VIM and NES in animals pretreated with stem-cell-like RUCM cells could in fact suggest that RUCM cells might have immunomodulatory properties, thereby altering the resultant astrogliotic response to CA. Anti-inflammatory effects due to intravenous infusion of umbilical-cord-blood-derived cells after ischemia have been demonstrated recently [38]. It is possible that umbilical-cord-matrix-derived cells have similar properties.

The lack of astroglial expression of VIM and significant reduction of NES in the RUCM cell-treated group may just be a sign of no or little permanent astroglial damage in these animals. It has been suggested [3] that the VIM^+ astroglia, but not $GFAP^+$ ones, correlate with permanent injury after ischemia. The re-expression of VIM and NES in reactive astrocytes is most commonly associated with a wide variety of brain injuries and always seen in the injured areas [3, 5, 29, 30, 39, 40]. The protection of astrocytes from permanent damage by stem-cell-like RUCM cells is consistent with and in support of the recent proposal [41] that the selective vulnerability of CA1 neurons is due to the selective vulnerability of the CA1 astrocytes. Stem-cell-like-cell protection of astroglial cells leads to the reduced long-term neuronal loss in the CA1 region.

Despite the strong correlations seen in Figure 7, the causal relationship between the presence of VIM re-expression and neural injury is, however, not clear. It has been suggested that VIM^+ astrocytes found in and around the injury are associated with hyperplasia and are representative of the newly formed immature astrocytes. Our data do not support this hypothesis because in the RUCM + CA group, while VIM^+ cells are almost absent, we do observe many $GFAP^+$ cells co-expressing Ki67 (Figure 6B), suggesting that these cells are either newly divided or in the process of division.

A recent study [4] suggested that VIM^+ astrocytes appeared to be correlated more with the cell migration than with cell proliferation. Reactive astrocytes expressing nestin have also been implicated in migration [42]. Re-expression of VIM in mature astrocytes may impart similar functions to them as radial glia [43]. Radial glia not only function as neural progenitors but also offer a scaffold to guide and support migrating neuroblasts. Supporting this is the observation [44] that the newly divided ($BrdU^+$) progenitor

cells were always found to be in close association with VIM+ astrocytes, but not co-localized with them. The VIM expression observed in Group 1 (CA only) and Group 2 (DM + CA) may be guiding the migration of neural precursors or microglia and macrophages to the site of lesion, and the stem-cell-like RUCM cell treatment (Group 3) prevents the damage or inflammation, thereby suppressing the signals for the cell migration. Our RCA-1 staining seems to support this conclusion.

Another possible explanation for the lack of VIM+ and reduction in NES+ reactive astrocytes is that the stem-cell-like RUCM cells release messenger molecules that inhibit the formation of glial scars. The Wharton's jelly, from which RUCM cells are isolated, has been shown to contain high concentrations of a wide variety of growth factors and cytokines [45]. VIM+ and NES+ reactive astrocytes are almost always reported to be in and around areas of glial scarring, and it has been demonstrated that glial scarring is an impediment to axonal regeneration post-injury [7, 46, 47]. The glial scar formation has been shown to be reduced or ablated when the expression of VIM is reduced by anti-sense expression or VIM and GFAP are eliminated in knock-out mice [48, 49]. It has also been shown [50] that the glial scar formation is modulated through the endothelin B receptor on reactive astrocytes. The expression of endotherlin B receptor in astrocytes has been shown to be dependent on both VIM and GFAP expression [51]. Therefore, it is possible that preventing VIM expression can result in the inhibition of glial scar formation, leading to the regeneration of axons for the survival of the CA1 neurons.

Conclusion

It is clear from our GFAP immunostaining that treatment with stem-cell-like RUCM cells prior to cardiac arrest does not inhibit the reactive astrocytosis normally associated with cerebral ischemia. It does, however, prevent the appearance of VIM+ reactive astrocytes and reduce NES+ reactive astrocytes in the selectively vulnerable CA1 regions, suggesting the possibility that the stem-cell-like RUCM cells prevent permanent astroglial damage. The large reduction in microglial activation and altered distribution suggests that RUCM cell transplantation has immunomodulatory effects. Combined, stem-cell-like RUCM cells offer protection against neuronal injury after global cerebral ischemia by enhancing the survivability of the astroglia in the selectively vulnerable regions.

Acknowledgement

The authors would like to thank Dr. Kathy Mitchell for providing the RUCM cells and Mr. Marc Uy for early participation in the stem cell transplantation experiments. This work was supported in part by a grant from NINDS and NHLBI (R01NS/HL036124).

References

1. Becker KJ. Targeting the central nervous system inflammatory response in ischemic stroke. Curr Opin Neurol. 2001;14:349-353.
2. Danton GH, Dietrich WD. Inflammatory mechanisms after ischemia and stroke. J Neuropathol Exp Neurol. 2003;62:127-136.
3. Petito CK, Morgello S, Felix JC, et al. The two patterns of reactive astrocytosis in postischemic rat brain. J Cereb Blood Flow Metab. 1990;10:850-859.
4. Wang Q, Tang XN, Yenari MA. The inflammatory response in stroke. J Neuroimmunol. 2007;184:53-68.
5. Pekny M, Nilsson M. Astrocyte activation and reactive gliosis. Glia. 2005;50:427-434.
6. Pekny M, Johansson CB, Eliasson C, et al. Abnormal reaction to central nervous system injury in mice lacking glial fibrillary acidic protein and vimentin. J Cell Biol. 1999;145:503-514.
7. Davies SJ, Goucher DR, Doller C, et al. Robust regeneration of adult sensory axons in degenerating white matter of the adult rat spinal cord. J Neurosci. 1999;19:5810-5822.
8. Wood PL. Microglia as a unique cellular target in the treatment of stroke: potential neurotoxic mediators produced by activated microglia. Neurol Res. 1995;17:242-248.

9. Cai Z, Lin S, Fan LW, et al. Minocycline alleviates hypoxic-ischemic injury to developing oligodendrocytes in the neonatal rat brain. Neuroscience. 2006;137:425-435.
10. Zhang N, Komine-Kobayashi M, Tanaka R, et al. Edaravone reduces early accumulation of oxidative products and sequential inflammatory responses after transient focal ischemia in mice brain. Stroke. 2005;36:2220-2225.
11. Yrjanheikki J, Tikka T, Keinanen R, et al. A tetracycline derivative, minocycline, reduces inflammation and protects against focal cerebral ischemia with a wide therapeutic window. Proc Natl Acad Sci U S A. 1999;96:13496-13500.
12. Yrjanheikki J, Keinanen R, Pellikka M, et al. Tetracyclines inhibit microglial activation and are neuroprotective in global brain ischemia. Proc Natl Acad Sci U S A. 1998;95:15769-15774.
13. Watanabe H, Abe H, Takeuchi S, et al. Protective effect of microglial conditioning medium on neuronal damage induced by glutamate. Neuroscience letters. 2000;289:53-56.
14. Capone C, Frigerio S, Fumagalli S, et al. Neurosphere-derived cells exert a neuroprotective action by changing the ischemic microenvironment. PLoS ONE. 2007;2:e373.
15. Hayashi Y, Tomimatsu Y, Suzuki H, et al. The intra-arterial injection of microglia protects hippocampal CA1 neurons against global ischemia-induced functional deficits in rats. Neuroscience. 2006;142:87-96.
16. Jomura S, Uy M, Mitchell K, et al. Potential treatment of cerebral global ischemia with Oct-4+ umbilical cord matrix cells. Stem Cells. 2007;25:98-106.
17. Troyer DL, Weiss ML. Wharton's jelly-derived cells are a primitive stromal cell population. Stem Cells. 2008;26:591-599.
18. Mitchell KE, Weiss ML, Mitchell BM, et al. Matrix cells from Wharton's jelly form neurons and glia. Stem Cells. 2003;21:50-60.
19. Liachenko S, Tang P, Hamilton RL, et al. A reproducible model of circulatory arrest and remote resuscitation in rats for NMR investigation. Stroke. 1998;29:1229-1238; discussion 1238-1229.
20. Liachenko S, Tang P, Hamilton RL, et al. Regional dependence of cerebral reperfusion after circulatory arrest in rats. J Cereb Blood Flow Metab. 2001;21:1320-1329.
21. Liachenko S, Tang P, Xu Y. Deferoxamine improves early postresuscitation reperfusion after prolonged cardiac arrest in rats. J Cereb Blood Flow Metab. 2003;23:574-581.
22. Xu Y, Liachenko S, Tang P. Dependence of early cerebral reperfusion and long-term outcome on resuscitation efficiency after cardiac arrest in rats. Stroke. 2002;33:837-843.
23. Young WL, Lawton MT, Gupta DK, et al. Anesthetic management of deep hypothermic circulatory arrest for cerebral aneurysm clipping. Anesthesiology. 2002;96:497-503.
24. Pekny M, Wilhelmsson U, Bogestal YR, et al. The role of astrocytes and complement system in neural plasticity. Int Rev Neurobiol. 2007;82:95-111.
25. Amir G, Ramamoorthy C, Riemer RK, et al. Neonatal brain protection and deep hypothermic circulatory arrest: pathophysiology of ischemic neuronal injury and protective strategies. Ann Thorac Surg. 2005;80:1955-1964.
26. Augoustides JG, Pochettino A, Ochroch EA, et al. Clinical predictors for prolonged intensive care unit stay in adults undergoing thoracic aortic surgery requiring deep hypothermic circulatory arrest. J Cardiothorac Vasc Anesth. 2006;20:8-13.
27. Kleisli T, Raissi SS, Nissen NN, et al. Cavo-atrial tumor resection under total circulatory arrest without a sternotomy. Ann Thorac Surg. 2006;81:1887-1888.
28. Strebel S, Mendelowitsch A, Kindler C. Rupture of a giant intracranial aneurysm while starting cardiopulmonary bypass for hypothermic circulatory arrest. J Neurosurg Anesthesiol. 2004;16:263-265.
29. Petito CK, Halaby IA. Relationship between ischemia and ischemic neuronal necrosis to astrocyte expression of glial fibrillary acidic protein. Int J Dev Neurosci. 1993;11:239-247.
30. Oblinger MM, Singh LD. Reactive astrocytes in neonate brain upregulate intermediate filament gene expression in response to axonal injury. Int J Dev Neurosci. 1993;11:149-156.
31. Sugawara T, Lewen A, Noshita N, et al. Effects of global ischemia duration on neuronal, astroglial, oligodendroglial, and microglial reactions in the vulnerable hippocampal CA1 subregion in rats. J Neurotrauma. 2002;19:85-98.
32. Briones TL, Woods J, Wadowska M, et al. Astrocytic changes in the hippocampus and functional recovery after cerebral ischemia are facilitated by rehabilitation training. Behav Brain Res. 2006;171:17-25.
33. Beamer CA, Brooks DM, Lurie DI. Motheaten (me/me) mice deficient in SHP-1 are less susceptible to focal cerebral ischemia. J Neurosci Res. 2006;83:1220-1230.
34. Lin CH, Cheng FC, Lu YZ, et al. Protection of ischemic brain cells is dependent on astrocyte-derived growth factors and their receptors. Exp Neurol. 2006;201:225-233.
35. Li L, Lundkvist A, Andersson D, et al. Protective role of reactive astrocytes in brain ischemia. J Cereb Blood Flow Metab. 2007.
36. Pei Z, Cheung RT. Pretreatment with melatonin exerts anti-inflammatory effects against ischemia/reperfusion injury in a rat middle cerebral artery occlusion stroke model. J Pineal Res. 2004;37:85-91.
37. Weng YC, Kriz J. Differential neuroprotective effects of a minocycline-based drug cocktail in transient and permanent focal cerebral ischemia. Exp Neurol. 2007;204:433-442.

38. Vendrame M, Gemma C, de Mesquita D, et al. Anti-inflammatory effects of human cord blood cells in a rat model of stroke. Stem Cells Dev. 2005;14:595-604.
39. Kitamura O. Immunohistochemical investigation of hypoxic/ischemic brain damage in forensic autopsy cases. Int J Legal Med. 1994;107:69-76.
40. Baldwin SA, Scheff SW. Intermediate filament change in astrocytes following mild cortical contusion. Glia. 1996;16:266-275.
41. Ouyang YB, Voloboueva LA, Xu LJ, et al. Selective dysfunction of hippocampal CA1 astrocytes contributes to delayed neuronal damage after transient forebrain ischemia. J Neurosci. 2007;27:4253-4260.
42. Takahashi H, Matsumoto H, Kumon Y, et al. Expression of heparanase in nestin-positive reactive astrocytes in ischemic lesions of rat brain after transient middle cerebral artery occlusion. Neuroscience letters. 2007;417:250-254.
43. Leavitt BR, Hernit-Grant CS, Macklis JD. Mature astrocytes transform into transitional radial glia within adult mouse neocortex that supports directed migration of transplanted immature neurons. Experimental Neurology. 1999;157:43-57.
44. Alonso G. Proliferation of progenitor cells in the adult rat brain correlates with the presence of vimentin-expressing astrocytes. Glia. 2001;34:253-266.
45. Sobolewski K, Malkowski A, Bankowski E, et al. Wharton's jelly as a reservoir of peptide growth factors. Placenta. 2005;26:747-752.
46. Alonso G, Privat A. Reactive astrocytes involved in the formation of lesional scars differ in the mediobasal hypothalamus and in other forebrain regions. J Neurosci Res. 1993;34:523-538.
47. Cho KS, Yang L, Lu B, et al. Re-establishing the regenerative potential of central nervous system axons in postnatal mice. J Cell Sci. 2005;118:863-872.
48. Lin J, Cai W. Effect of vimentin on reactive gliosis: in vitro and in vivo analysis. J Neurotrauma. 2004;21:1671-1682.
49. Ribotta MG, Menet V, Privat A. Glial scar and axonal regeneration in the CNS: lessons from GFAP and vimentin transgenic mice. Acta Neurochir Suppl. 2004;89:87-92.
50. Rogers SD, Peters CM, Pomonis JD, et al. Endothelin B receptors are expressed by astrocytes and regulate astrocyte hypertrophy in the normal and injured CNS. Glia. 2003;41:180-190.
51. Wilhelmsson U, Li L, Pekna M, et al. Absence of glial fibrillary acidic protein and vimentin prevents hypertrophy of astrocytic processes and improves post-traumatic regeneration. J Neurosci. 2004;24:5016-5021.

Figure 1. (A) Representative hippocampal CA1 sections immunochemically stained for both GFAP and VIM immunoactivities. Horizontal bar represents 150 μm. (B) Bar graphs summarizing the percent GFAP$^+$ areas, GFAP$^+$ cells densities, and VIM$^+$ cell counts in the contralateral and injection sides, averaged for each of the six experimental groups (see text for details). Pink, cyan, and yellow bars represent no pretreatment (or sham), DM injection, and RUCM cell transplantation, respectively. Notice the pronounced reduction in the appearance of VIM$^+$ astrocytes after 8-min cardiac arrest and 7-day recovery in the animals treated with stem-cell-like RUCM cells. *, $p < 0.05$; **, $p < 0.01$.

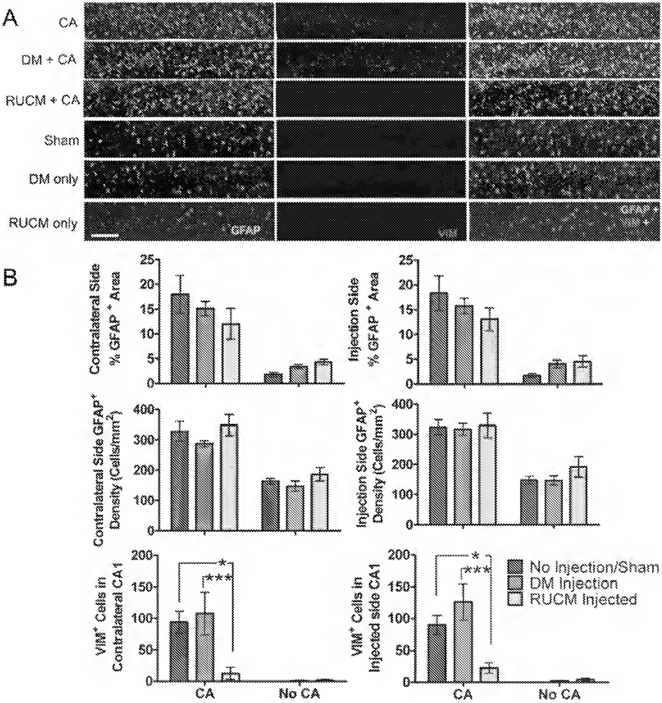

Figure 2. GFAP (Ggreen) staining at the 20× magnification showing increased staining within the hippocampal CA1 regions for all experimental groups with 8-min cardiac arrest. Notice the thicker and more numerous astrocytic processes. Blue color shows the nuclear stain for DAPI.

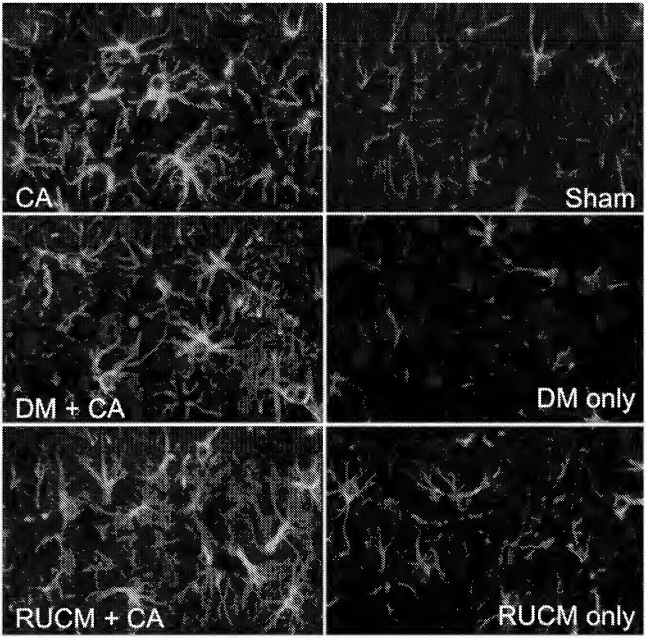

Figure 3. (A) Representative CA1 sections stained for Nestin. Astrocytes show Nestin$^+$ expression in rats that were subjected to 8-min of cardiac arrest. Photomicrographs were obtained at 10× magnification. Bar represents 150 μm. (B) Bar graphs summarizing the percent Nestin$^+$ areas in the contralateral and injection sides averaged for each of the six experimental groups. Pink, cyan, and yellow bars represent no pretreatment (or sham), DM injection, and RUCM cell transplantation, respectively. Treatment with stem-cell-like RUCM cells 3 days before cardiac arrest greatly reduced the amount of nestin$^+$ astrocytes in the CA1 region of the hippocampus. ***, P = 0.003.

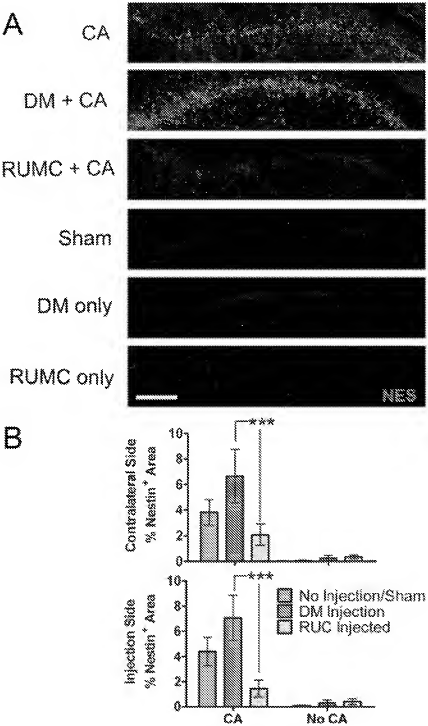

Figure 4. (A) Representative CA1 sections stained for microglia using RCA-1. Microglia appear as darkly stained cells while neurons appear as white spots. All rats subjected to 8-min cardiac arrest show the appearance of microglia. Photomicrographs were obtained at 10× magnification. Bar represents 150 μm. (B) Bar graphs summarizing the percent RCA-1$^+$ areas in the contralateral and injection sides, averaged for each of the six experimental groups. Pink, cyan, and yellow bars represent no pretreatment (or sham), DM injection, and RUCM cell transplantation, respectively. Pretreatment with stem-cell-like RUCM cells reduces the RCA-1$^+$ area and changes their distribution. ***, P < 0.001.

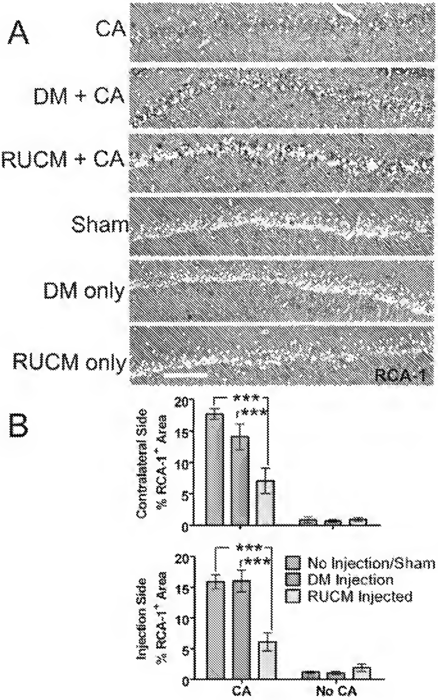

Figure 5. (A) Representative sections in the CA1 region of the hippocampus stained for Ki67. Photomicrographs were obtained at 10× magnification. The scale bar represents 150 μm. (B) Bar graphs summarizing the Ki67^{+} cell counts in the contralateral and injection sides, averaged for each of the six experimental groups. Pink, cyan, and yellow bars represent no pretreatment (or sham), DM injection, and RUCM cell transplantation, respectively. Eight minute cardiac arrest, irrespective of treatment, increases the number of Ki67^{+} cells.

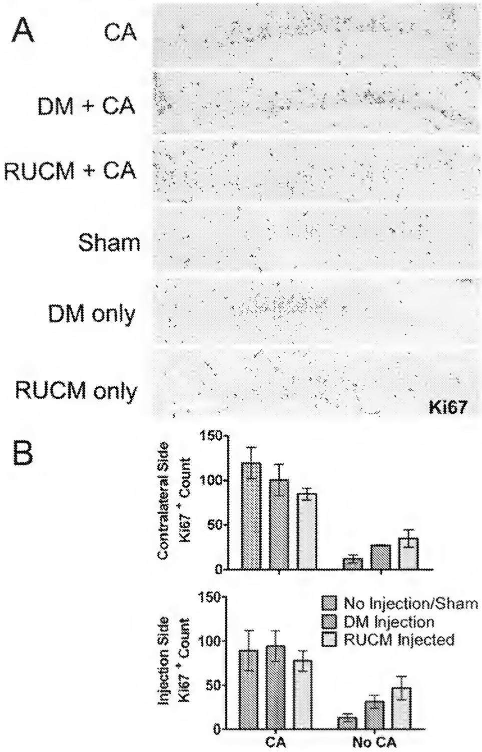

Figure 6. High-magnification (60×), maximum-intensity projection of 6-μm-thick image stacks showing co-localization of (A) IBA-1+ microglia (red) expressing Ki67 (green) and (B) GFAP+ astrocytes (green) expressing Ki67 (red) in the CA1 region of the rat hippocampus after 8-min cardiac arrest and 7-day reperfusion.

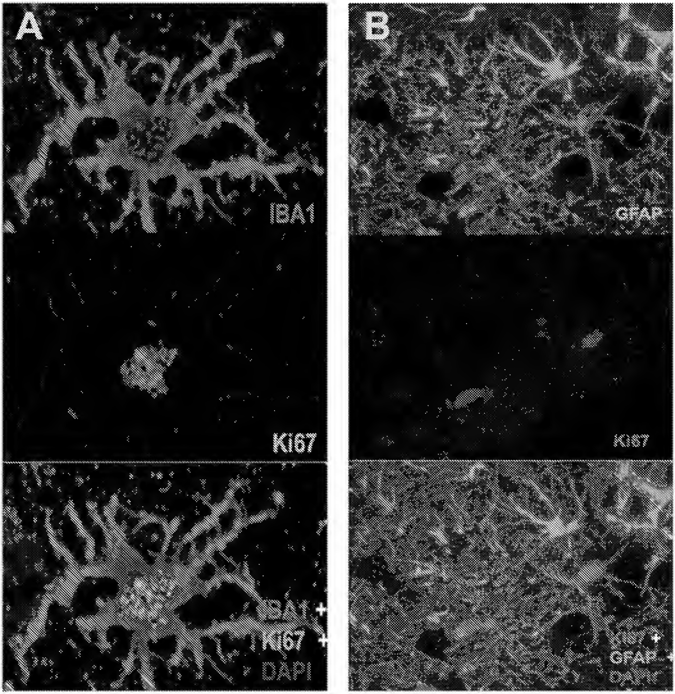

Figure 7. Correlations between percentage of the hippocampal CA1 neuronal loss and (A) VIM+ cells or (B) activated microglia. Data are taken from the within-group averages from the contralateral (●) and injection (▲) sides of the six experimental groups as detailed in the text.

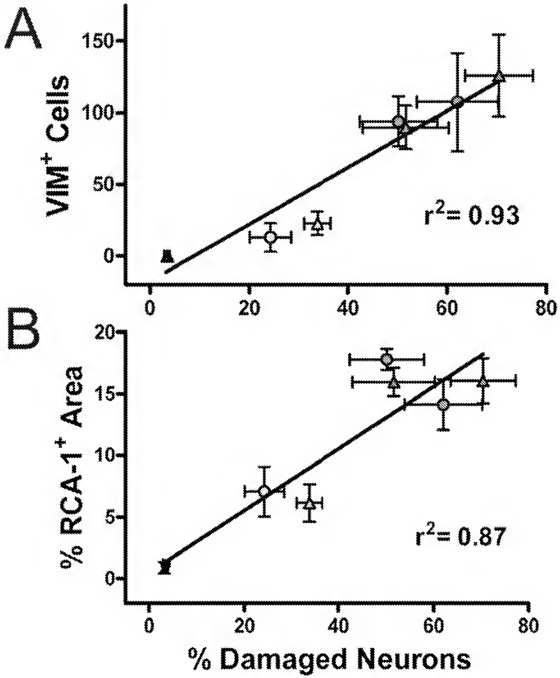

TAB 2

STEM CELLS®

Potential Treatment of Cerebral Global Ischemia with Oct-4+ Umbilical Cord Matrix Cells

Sachiko Jomura, Marc Uy, Kathy Mitchell, Renee Dallasen, Claudia J. Bode and Yan Xu

Stem Cells 2007;25;98-106; originally published online Sep 7, 2006;
DOI: 10.1634/stemcells.2006-0055

STEM CELLS®, an international peer-reviewed journal, covers all aspects of stem cell research: embryonic stem cells; tissue-specific stem cells; cancer stem cells; the stem cell niche; stem cell genetics and genomics; translational and clinical research; technology development.

STEM CELLS® is a monthly publication, it has been published continuously since 1983. The Journal is owned, published, and trademarked by AlphaMed Press, 318 Blackwell Street, Suite 260, Durham, North Carolina, 27701. © 2007 by AlphaMed Press, all rights reserved. Print ISSN: 1066-5099. Online ISSN: 1549-4918.

AlphaMed Press

STEM CELLS®

TISSUE-SPECIFIC STEM CELLS

Potential Treatment of Cerebral Global Ischemia with Oct-4^{+} Umbilical Cord Matrix Cells

SACHIKO JOMURA,[a] MARC UY,[a] KATHY MITCHELL,[c] RENEE DALLASEN,[a] CLAUDIA J. BODE,[c] YAN XU[a,b]

[a]Department of Anesthesiology, University of Pittsburgh School of Medicine, Pittsburgh, Pennsylvania, USA;
[b]Department of Pharmacology, University of Pittsburgh School of Medicine, Pittsburgh, Pennsylvania, USA;
[c]Department of Pharmacology and Toxicology, University of Kansas, Lawrence, Kansas, USA

Key Words. Cerebral global ischemia • Rat umbilical cord matrix cell • Oct-4 • Extracellular signaling • Neurogenesis • Reperfusion
Stem cell therapy

ABSTRACT

Potential therapeutic effects of Oct-4-positive rat umbilical cord matrix (RUCM) cells in treating cerebral global ischemia were evaluated using a reproducible model of cardiac arrest (CA) and resuscitation in rats. Animals were randomly assigned to four groups: A, sham-operated; B, 8-minute CA without pretreatment; C, 8-minute CA pretreated with defined media; and D, 8-minute CA pretreated with Oct-4^{+} RUCM cells. Pretreatment was done 3 days before CA by 2.5-μl microinjection of defined media or approximately 10^{4} Oct-4^{+} RUCM cells in left thalamic nucleus, hippocampus, corpus callosum, and cortex. Damage was assessed histologically 7 days after CA and was quantified by the percentage of injured neurons in hippocampal CA1 regions. Little damage (approximately 3%–4%) was found in the sham group, whereas 50%–68% CA1 pyramidal neurons were injured in groups B and C. Pretreatment with Oct-4^{+} RUCM cells significantly (p < .001) reduced neuronal loss to 25%–32%. Although the transplanted cells were found to have survived in the brain with significant migration, few were found directly in CA1. Therefore, transdifferentiation and fusion with host cells cannot be the predominant mechanisms for the observed protection. The Oct-4^{+} RUCM cells might repair nonfocal tissue damage by an extracellular signaling mechanism. Treating cerebral global ischemia with umbilical cord matrix cells seems promising and worthy of further investigation. STEM CELLS *2007;25:98–106*

INTRODUCTION

Unless resuscitation is given immediately, cardiac arrest (CA) invariably leads to debilitating brain damage and death due to cessation of oxygen and glucose supply to the brain tissue. Injury patterns after cerebral global ischemia are characterized by the disseminated neuronal loss of the selectively vulnerable pyramidal neurons in the CA1 and CA3 regions of the hippocampus, medium-sized neurons in the striatum, and Purkinje cells in cerebellum [1–4]. Even with a brief primary insult, the selectively vulnerable neurons die hours to days after the ischemia. For a long time, the secondary derangements were thought to be the direct consequence of excitotoxicity and energy failure. More recent investigations [1–3, 5–8], however, suggest that treatment strategies aimed simply at energy metabolism or excitotoxicity would inevitably fail. Finding alternative strategies to rescue injured neurons from dying and to help uninjured neurons to survive has been the subject of intense investigations in recent years [9–11]. One of the possibilities is to promote neurogenesis from neural stem cells and progenitor cells in the adult brain [12]. It has been suggested that neurogenesis is enhanced by transient brain ischemia [13–17]. Moreover, neurotrophic factors are believed to play an important role in this mechanism. Levels of neurotrophic factors such as brain-derived neurotrophic factor [18–20], fibroblast growth factor-2 [21], and erythropoietin [22] in the brain have been shown to increase after ischemic injury. These neurotrophic factors have also been used for experimental treatment of brain ischemia.

Another way to promote neurogenesis and neuronal protection is stem cell transplantation. Several attempts have been made to use stem cells from different origins [23], including bone marrow stem cells [24–26], neuroepithelical stem cells [27], fetal neural stem cells [28], and umbilical cord blood cells [29, 30], for treatment of focal ischemia. These studies showed the migration and differentiation of stem cells in relation to the functional recovery. Some recent studies even suggest that stem cell contributions to organ repair can arise from a circulating pool of the adult bone marrow stromal stem cells because cells from the donor marrow can be found in the brain, liver, kidney, or lung [31–34]. The potential therapeutic application of stem cell factor to focal ischemia was also investigated [35]. Very few studies to date, however, have focused on the use of stem cells for the treatment of global cerebral ischemia due to the dispersed nature of the damage. The possibility of treating cerebral global ischemia with exogenous stem cells has not yet been fully explored.

In the present study, we combined the use of rat umbilical cord matrix (RUCM) cells and a clinically relevant outcome model of CA and resuscitation in rats [1, 2] to investigate the potential therapeutic effects of Oct-4^{+} RUCM cells in mitigating cerebral global ischemic damage after 8-minute normothermic CA.

Correspondence: Yan Xu, Ph.D., University of Pittsburgh School of Medicine, Biomedical Science Tower 3, Room 2048, 3501 Fifth Avenue, Pittsburgh, Pennsylvania 15260, USA. Telephone: 412-648-9922; Fax: 412-648-8998; e-mail: xuy@anes.upmc.edu Received January 26, 2006; accepted for publication August 29, 2006; first published online in STEM CELLS *EXPRESS* September 7, 2006. ©AlphaMed Press 1066-5099/2007/$20.00/0 doi: 10.1634/stemcells.2006-0055

Materials and Methods

Isolation and Culture of RUCM Cells

RUCM cells were isolated from the umbilical cords of female Sprague-Dawley rats at 16-day gestation in accordance with a protocol approved by the Institutional Animal Care and Use Committee (IACUC) at University of Kansas (Lawrence, KS). The procedure is similar to that used for isolating porcine and human UCM cells [36]. Briefly, cords were washed in betadine, rinsed in sterile phosphate-buffered saline (PBS), incubated in hyaluronidase (40 U/ml) (MP Biomedicals, Solon, OH, http://www.mpbio.com) and collagenase type I (0.4 mg/ml) (Sigma-Aldrich, St. Louis, http://www.sigmaaldrich.com) for 30 minutes at 37°C, and rinsed with sterile PBS. Cords were finely minced, plated in six-well plates, and maintained in defined media (DM), which are composed of Dulbecco's modified Eagle's medium (Invitrogen, Carlsbad, CA, http://www.invitrogen.com) and MCDB-201 medium (Sigma-Aldrich) supplemented with 1× insulin-transferrin-selenium (Invitrogen), 0.15% lipid-rich bovine serum albumin (Albumax; Invitrogen), 0.1 nM dexamethasone (Sigma-Aldrich), 10 μM ascorbic acid-2-phosphate (Sigma-Aldrich), 1× penicillin/streptomycin (Thermo-Fisher, Suwanee, GA, http://new.fishersci.com), 2% fetal bovine serum (BD Biosciences, San Jose, CA, http://www.bdbiosciences.com), 10 ng/ml recombinant human epidermal growth factor, and 10 ng/ml rat platelet-derived growth factor BB (R&D Systems, Inc., Minneapolis, http://www.rndsystems.com). On day 5, cord remnants were removed, and the attached cells were washed three times with PBS, followed by addition of fresh DM. Cells were passaged by lifting with 0.05% trypsin EDTA. Viable cells were counted with a hemocytometer and trypan blue exclusion and usually replated at an initial density of 30%. Cells were passaged when they reached 80% confluency.

Flow Cytometry

RUCM cells at 1×10^6 cells per milliliter were fixed with methanol at 4°C for 5 minutes and blocked with PBS and 5% bovine serum albumin at 4°C for 1 hour. Cells were incubated with mouse primary antibodies (1 μg/ml) against Oct-4, smooth muscle actin (SMA), or vimentin (Chemicon International, Temecula, CA, http://www.chemicon.com) at 4°C for 1 hour. Cells were then washed three times with PBS and incubated with goat anti-mouse secondary FITC conjugate (1:100, Invitrogen) for 30 minutes at 4°C. Thereafter, cells were washed twice in PBS and analyzed using a FACSCalibur flow cytometer (Beckman Coulter, Fullerton, CA, http://www.beckmancoulter.com). Ten-thousand cells (no gating) were collected and analyzed in the FL1 channel. Control cells were incubated with mouse isotype-specific immunoglobulin G to establish the background signal.

Reverse Transcription-Polymerase Chain Reaction Analyses

RNA was isolated from cultured RUCM cells with RNeasy Quick spin columns (Qiagen Inc., Valencia, CA, http://www1.qiagen.com) and converted to cDNA using random hexamers and SuperScript II reverse transcriptase (Invitrogen). Polymerase chain reaction (PCR) amplification was performed using a Bio-Rad I-Cycler (Bio-Rad, Hercules, CA, http://www.bio-rad.com) for 35 cycles with the following primer pairs: Oct-4, forward 5′-GAAGGATGTGGTCCGAGTGT-3′, reverse 5′-GTGAAGTGAGGGCTCCCATA-3′ (expected product size of 183 base pair [bp]); vimentin, forward 5′-ATGTCCACCAGGTCCGTG-3′, reverse 5′-TTATTCAAGGTCATCGTG-3′ (expected product size of 1.4 kbp); and glyceraldehyde-3-phosphate dehydrogenase (GAPDH, as a positive control), forward 5′-ATCTTCCAGGAGCGAGAT-3′ and reverse 5′-TGGTCATGAGTCCTTCCACGATA-3′ (expected product size of 380 bp). For negative control, PCR was performed in the presence of cDNA but without primers. Products were resolved by 2% agarose gel electrophoresis and visualized by ethidium bromide staining.

Immunofluorescence

RUCM cells from passage 10 were grown to 80% confluency in chamber slides. Cells were fixed with 4% paraformaldehyde for 10 minutes at room temperature, quenched in 100 mM glycine for 5 minutes, permeabilized with 0.2% Triton X-100 for 5 minutes, and blocked in blocking buffer (0.2% Triton X-100, 2% normal goat serum, 0.4% bovine serum albumin in PBS) for 1 hour. Cells were incubated with primary antibody for 1 hour (mouse monoclonal antibodies to Oct-4 and SMA, 1:100, Chemicon). Cells were washed three times with PBS and incubated with secondary antibody (Alexa Fluor 546 donkey anti-mouse, 1:200, Invitrogen) for 1 hour. Nuclear DNA was stained with SYTOX Blue nucleic acid stain (Invitrogen). For negative controls, cells were incubated with the labeled secondary antibodies and SYTOX Blue only. Images were obtained with a 510 Zeiss laser scanning microscope (Carl Zeiss, Jena, Germany, http://www.zeiss.com) under ×63 oil-immersion lens.

In Vivo Experimental Groups

The CA and resuscitation procedures were approved by the IACUC at the University of Pittsburgh. Thirty-three male Sprague-Dawley rats (Harlan Sprague Dawley, Inc., Indianapolis, http://www.harlan.com), weighing 234 ± 27 g, were used. Rats were randomized into four groups. In group A (sham-operated, $n = 7$), rats were subjected to the same surgical and CA and resuscitation procedures as detailed below but were resuscitated immediately after the induction of CA without asphyxia. In groups B ($n = 9$), C ($n = 9$), and D ($n = 8$), rats underwent 8 minutes of CA, followed by rapid resuscitation. Rats in group C and group D were pretreated 3 days prior to CA with an intracranial microinjection of sterilized defined cell culture medium and RUCM cells, respectively. In all groups, the rat body temperature was measured by a rectal temperature probe and controlled to 36.5°C ± 0.5°C throughout the experiment using a heating pad and warm light source.

CA and Resuscitation

Rats were prepared as described previously [1, 2] with a few minor modifications. Under approximately 3% isoflurane anesthesia, rats were quickly intubated orotracheally. After intubation, rats were mechanically ventilated with a 50:50 mixture of air and O_2. Anesthesia was maintained with 1.5%–2% isoflurane, and paralysis was produced by pancuronium bromide (2 mg/kg). The arterial blood pH and gases were measured using a Ciba-Corning blood gas analyzer (model 278; Bayer HealthCare, Tarrytown, NY, http://www.bayerdiag.com) or an i-STAT portable clinical analyzer (Abbott Laboratories, Abbott Park, IL, http://www.abbott.com). Ventilation rate (1 ml/100 g of body weight, 40–45 strokes per minute) and positive end-expiratory pressure were carefully adjusted to control the arterial blood gas values in the normal range before CA [1, 3, 8]. Both femoral arteries and the left femoral vein were catheterized. One of the arterial catheters was used for continuous monitoring and recording of arterial blood pressure and heart rate. The other was used for arterial blood sampling and later for retrograde infusion of oxygenated blood during resuscitation. Approximately 15 minutes before CA, ventilation was switched to 100% oxygen and approximately 5 minutes later, oxygenated blood was withdrawn from the same rat. To prevent spontaneous breathing during the asphyxial CA, a booster dose of short-acting muscle relaxant (vecuronium bromide, 1 mg/kg) was injected intravenously 3 minutes before CA. CA was induced by asphyxia (stoppage of mechanical ventilation) combined with an i.v. bolus injection of an ultra-short-acting β_1-blocker, esmolol (6.25 mg). The later ensures a very tight control of the time from the onset of asphyxia to the electromechanical dissociation leading to circulatory arrest. Isoflurane anesthesia was discontinued during CA. Resuscitation was started 8 minutes after the induction of CA by 100% O_2 ventilation along with retrograde infusion of oxygenated blood mixed with the resuscitation mixture containing heparin (5 U/ml), sodium bicarbonate (0.05 mEq/ml), and epinephrine (8 μg/ml) through one of the catheterized femoral arteries into the abdominal and thoracic aorta. Infusion was performed manually to maintain the mean arterial blood pressure approximately 40 mmHg and was stopped at the first sign of

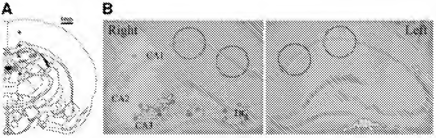

Figure 1. Anatomic references. (A): The microinjection sites, as marked by the gray dots, for rat umbilical cord matrix cell transplantations. The stereotactic coordinates are 1 mm left and 2.1 mm posterior to the bregma and 1.5 mm (cortex), 2.6 mm (corpus callosum), 3.5 mm (dorsal hippocampal region), and 5.0 mm (dorsal thalamic nucleus) from the top of the brain. (B): Cresyl violet staining of a rat brain section at the dorsal hippocampus level showing the predetermined areas (circles) in the CA1 regions where neuronal counting was performed. Abbreviations: CC, corpus callosum; DG, dentate gyrus; DV3, dorsal third ventricle; LV, lateral ventricle.

resumption of spontaneous circulation (ROSC). The rats were continually ventilated for at least 2 hours with anesthesia reinstated as required. Thereafter, arterial and venous catheters were surgically removed, and the wound was closed. Mechanical ventilation with air was continued until the effects of muscle relaxant subsided and sustained spontaneous breathing was observed. Animals were then extubated and returned to individual cages for postresuscitation evaluation for 7 days.

Stem Cell Transplantation

RUCM cells were obtained and cultured in the same way as described above. To ensure that a clonal population of cells was transplanted, RUCM cells at passage 53 were plated in 96-well plates with cell densities approximately 1 cell per well. After several days of culturing, cells from a single well were slowly expanded and harvested at passages 67, 69, 96, or 97 for transplantation. Chromosome analysis was done at passage 61 and 78 to confirm that cells from these passages have the same composite karyotype. Immunohistostaining and reverse transcription (RT)-PCR were repeated to confirm that these cells remained Oct-4-positive. Sixteen hours before transplantation, cells were labeled with 5 μM green fluorescent carboxyfluorescein diacetate (CFDA) (Invitrogen) for later histology tracking. Once inside the cells, the CFDA dye is converted to anionic CFDA succinimidyl ester (CFDA-SE) by intracellular esterases and couples to amine groups on proteins to achieve long-term intracellular labeling. Thus, after the acetate groups are cleaved off, CFDA-SE dye can be transferred to other (or daughter) cells only through cell division or cell fusion.

Rats were anesthetized with isoflurane and placed on a stereotactic apparatus for precise intracranial microinjection. Using predetermined coordinates based on the Paxinos atlas [37], the CFDA-labeled RUCM cells were injected into the following four sites in the left hemisphere: dorsal thalamic nucleus (DTN), dorsal hippocampus (H), corpus callosum (CC), and dorsal cortex (Fig. 1A). Because injuries after global ischemia are disseminated, these sites are selected based either on their vulnerability to ischemia or on their ability to allow cell migration. Approximately 4×10^5 cells in 10 μl (2.5 μl at each site) were transplanted at an infusion rate of 0.1 μl/minute using a programmable infusion pump (model UMC4; World Precision Instruments, Inc., Sarasota, FL, http://www.wpiinc.com) and a Mity Flexfil-microsyringe (model 500,818; World precision Instruments, Inc.) with a 200-μm outer diameter flexi-tip titanium needle. After transplantation, the needle was left in the brain for an additional 15 minutes before removal. As a negative control of the transplantation procedure, rats in group C received microinjections of the same volume of DM at exactly the same four coordinates. Three days after the cell transplantation or DM injection, the CA procedure was performed.

Outcome Evaluation

Rats were observed for 7 days after CA and resuscitation. The functional recovery was evaluated using the neurological deficit scores (NDS), which have a value ranging from 0 for brain death to 500 for neurologically normal, as detailed previously [1, 38]. After final NDS evaluation, rats were anesthetized with isoflurane and perfused with buffered 10% formalin phosphate. The brain was extracted from the skull and stored in buffered 10% formalin for 48 hours. The brain section containing the dorsal hippocampal region was embedded in paraffin and sliced into 6-μm-thick coronal sections. Alternating sections were stained with cresyl violet to visualize neuronal damages and deparaffinized to evaluate the survival, engraftment, and migration of the transplanted RUCM cells by the fluorescence microscopy of CFDA. The dorsal hippocampus of coronal sections was photographed. To quantify the histology damages, normal and damaged neurons were counted using Adobe Photoshop software (Adobe Systems Incorporated, San Jose, CA, http://www.
adobe.com) in four predetermined regions (two in each hemisphere) in the CA1 of the coronal hippocampal sections between 3.3 and 3.6 mm posterior to the bregma (Fig. 1B). Each circled region in the hippocampus had, on average, 89 ± 21 neurons. Every region was counted by at least two investigators who were blinded of the treatment groups to minimize bias in judgment. The histology damage was quantified as the percentage of damaged neurons against the total neuronal counts in the same region.

Three-Dimensional Rendering of Cell Migration

To better visualize the fate of transplanted RUCM cells, three-dimensional (3D) reconstruction of cell migration was rendered using a total of 114 consecutive coronal sections (thickness 6 μm) from the brain of a typical cell-transplanted rat, killed 7 days after CA and 10 days after transplantation. The sections were serially prepared using a microtome and were digitally imaged using a Leica DMR fluorescence microscope (Leica, Heerbrugg, Switzerland, http://www.leica.com) to visualize the CFDA dye in the RUCM stem cells. The images were imported into the Reconstruct software [39] (http://www.synapses.bu.edu) and aligned using the ventricles and other physical structures as reference points. The height and width scale of the sections was determined by the Measure program in Leica software module and was used as a parameter to scale the images in Reconstruct. Each fluorescent stem cell in the brain sections was contoured using Reconstruct. The Paxinos rat brain atlas [37] was used as a reference for creating anatomical structural groups, including the lateral and third ventricles, the hippocampus, and the corpus callosum, to show the locations of the transplanted cells and their migration. The 3D surface reconstructions generated by Reconstruct were exported to 3D Studio MAX (Autodesk, Inc., San Rafael, CA, http://usa.autodesk.com) for final rendering.

Data Analysis

Statistical analysis was performed using the Origin software (OriginLab Corporation, Northampton, MA, http://www.originlab.com) and GraphPad PRISM (GraphPad Software, Inc., San Diego, http://www.graphpad.com). One-way analysis of variance was used to compare the physiological parameters (Table 1), and the Bonferroni multiple-comparison test was used to determine the differences among groups. A p value of $<.05$ was considered statistically significant. All data are reported as mean ± SD except for neuronal counting, which is presented as mean ± SE.

Table 1. Parameters of cardiac arrest and resuscitation

	No. of rats survived/total	Weight (g)	Time to CA (minutes)	Time to ROSC (minutes)	Duration of CA (minutes)	NDS (no. of rats)	MABP (mmHg) 15 minutes before CA	MABP (mmHg) 2 hours after ROSC
Group A	6/7	206 ± 21	0.33 ± 0.09	0.77 ± 0.33	0.99 ± 0.43	500 (6)	129 ± 14	120 ± 12
Group B	8/9	245 ± 28	0.40 ± 0.07	0.71 ± 0.15	8.28 ± 0.16	500 (8)	132 ± 15	109 ± 10
Group C	7/9	225 ± 14	0.39 ± 0.15	0.74 ± 0.10	8.32 ± 0.19	495 ± 5 (7)	126 ± 26	116 ± 27
Group D	8/8	257 ± 17	0.33 ± 0.04	0.60 ± 0.13	8.27 ± 0.13	499 ± 4 (8)	118 ± 12	108 ± 9

Abbreviations: CA, cardiac arrest; MABP, mean arterial blood pressure; NDS, neurologic deficit score; ROSC, return of spontaneous circulation.

Results

Characterization of RUCM Stem Cells

The typical morphology of RUCM cells in culture at passage 10 is shown in a bright-field micrograph in Figure 2A. The cell morphology and growth rate remained essentially the same at later passages. The nuclear localization of the embryonic transcription factor, Oct-4 (red), was demonstrated by its colocalization with SYTOX nuclear stain (blue) (Fig. 2B). The cytoplasmic localization of the SMA filaments (red) is shown in Figure 2C. The negative control sample with the secondary antibody only shows no immunoreactivity (Fig. 2D). Flow cytometry results obtained from one of four different isolations of RUCM cells are shown in Figure 2E. Oct-4 was expressed in nearly 90% of the total number of cells counted as determined by flow cytometry with an average of 87% ± 5% (±SD, $n = 4$) for the four different isolations of RUCM cells. SMA and vimentin were expressed by an average of 85% ± 11% ($n = 4$) and 80% ± 11% ($n = 4$) for the four different isolations of RUCM cells, respectively. Expression of vimentin and Oct-4 was determined by RT-PCR with GAPDH as a positive control. The negative control was done where PCR was performed in the presence of cDNA but no primers (Fig. 2F). PCR products of the expected sizes for Oct-4 and vimentin were detected.

Stem Cell Treatment of Global Cerebral Ischemia

CA and resuscitation were highly reproducible in all experimental groups subjected to 8-minute CA. Four out of 33 animals (one each in groups A and B, two in group C) died of unidentified causes before the end of the planned recovery period. None of the animals in group D with RUCM cell transplantation died unexpectedly. Table 1 summarizes the important parameters of CA and resuscitation. In groups B (untreated CA), C (CA pretreated with defined medium), and D (CA pretreated with RUCM cells), all rats showed the same arterial blood pressure changes as reported previously [1], and the arterial blood pH and gases were within the normal physiological range before CA (pH 7.43 ± 0.03, pCO_2 36.1 ± 3.1, SpO_2 99.7 ± 0.1). The esmolol injection induced a rapid onset of CA. The time from esmolol bolus injection to CA was 0.37 ± 0.10 minutes. No significant differences were detected among groups. There were no differences in the resuscitation time among groups B (untreated CA), C (CA pretreated with defined medium), and D (CA pretreated with RUCM cells). The time from the initiation of the resuscitation effort to ROSC in these three groups was 0.68 ± 0.14 minutes (0.70 ± 0.19 minutes for the four-group average and 0.77 ± 0.33 minutes for group A alone). In groups B, C, and D, 8 minutes elapsed between the esmolol injection and the onset of resuscitation. The actual duration of CA (from electromechanical dissociation to ROSC) was 8.29 ± 0.16 minutes, and there were no significant differences among the three groups. Rats in sham group (group A) were injected

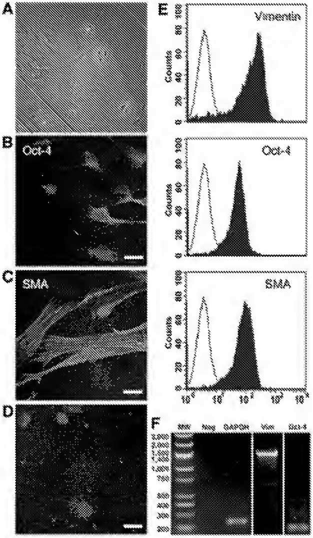

Figure 2. Characterization of rat umbilical cord matrix (RUCM) cells. Cells were imaged by **(A)** bright-field microscopy or immunostained for **(B)** Oct-4 and **(C)** smooth muscle actin (SMA) (red). Confocal images were overlaid with SYTOX Blue nucleic acid stain (blue). **(D):** Negative control with secondary antibody overlaid only with SYTOX Blue shows no immunoreactivity. **(E):** Flow cytometric analysis of RUCM cells. Each panel represents a single antibody assay. Black lines represent control cells with mouse immunoglobulin G alone plus fluorescein isothiocyanate-labeled secondary antibody. Black-filled lines represent primary mouse antibodies for vimentin, Oct-4, or SMA. **(F):** Reverse transcription-polymerase chain reaction of mRNA isolated from one representative RUCM cell line demonstrating the expression of the myofibroblast marker vimentin (Vim, 1.4 kilobase pair), the stem cell marker Oct-4 (183 base pair [bp]), and the housekeeping gene *GAPDH* (300 bp). The negative control (Neg) demonstrates the absence of product in a reaction with no added primers. Abbreviations: GAPDH, glyceraldehyde-3-phosphate dehydrogenase; MW, molecular weight.

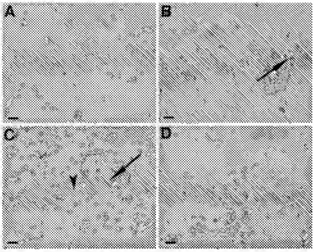

Figure 3. Representative cresyl violet-stained sections of the CA1 region of hippocampus from rats in groups A (sham-operated), B (untreated cardiac arrest), C (cardiac arrest pretreated with defined medium), and D (cardiac arrest pretreated with Oct-4⁺ rat umbilical cord matrix cells). Typical global ischemic damages, including vacuolization (arrow in frame B), nuclear pyknosis (arrow in frame C), and karyorhexis (arrowhead), are found in groups B, C, and D, but not in group A. The number of injured neurons is significantly reduced in group D compared with groups B and C. Scale bars = 20 μm.

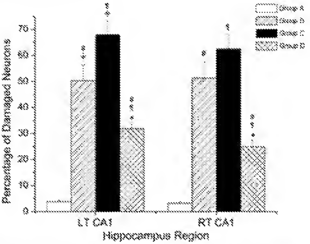

Figure 4. The histological damage, quantified by the percentage of injured neurons counted in the predetermined areas in the CA1 regions of the hippocampus (as shown in Fig. 1B). Results from one-way analysis of variance with Bonferroni multiple comparisons are marked: # and § indicate significant difference ($p < .001$) between groups of the same side; ‡ and * indicate significant difference ($p < .05$) between groups of the same side and within the same group of the opposite sides, respectively. Abbreviations: LT, left; RT, right.

with esmolol and resuscitated immediately by infusion of oxygenated blood and resuscitation mixture. The transient "no-flow" time for rats in group A was 0.99 ± 0.43 minutes. A larger standard deviation of no-flow time in group A compared with other groups was likely due to the varying responses to the possible drug interaction between esmolol and epinephrine when the short-action esmolol was still effective in the sham group while the resuscitation mixture was infused.

There was no specific ischemic damage in group A (sham group); neurons stained with cresyl violet show clear round nuclei and cell bodies in dark purple (Fig. 3A). Only 3.8% ± 0.5% and 3.2% ± 0.5% of the hippocampal neurons were damaged in the left and right CA1 regions, respectively. The same amount of "apparent damage" is also seen in animals without having CA surgical manipulations. Seven days after resuscitation, six out of seven animals in group A recovered fully with normal NDS (Table 1). Group B (untreated CA group) had typical ischemic changes in the CA1 neurons, including nuclear pyknosis (the condensation of chromatin), vacuolization (formation of large membrane-bound vacuoles), and karyorhexis (the fragmentation of the nucleus) (Fig. 3B, 3C), and 50.1% ± 6.0% and 51.3% ± 6.2% of the pyramidal neurons in the left and right CA1 regions were damaged, respectively. Despite severe histological damage, the rats that survived in group B showed normal NDS 7 days after resuscitation (Table 1). It is a characteristic finding that behavioral recovery from CA as measured by the NDS is often an all-or-none phenomenon: animals either die within days or appear neurologically normal [3]. Hence, histology outcome as measured by the neuronal loss in the CA1 region is a more quantifiable measure of the damage. CA1 neurons in group C (CA pretreated with DM) had slightly more severe damage than in group B, with 67.9% ± 5.5% and 62.4% ± 5.8% of neurons injured in the left and right CA1 regions, respectively (Fig. 4). The difference between group B (untreated CA) and group C (CA pretreated with DM) is significant only on the ipsilateral (injection) side ($p = .04$) and not significant on the contralateral side ($p = .20$). Four animals in group C were nonresponding to tail clamping 7 days after resuscitation (NDS 49.5 ± 5.3). The percentage of damaged hippocampus neurons in group D (CA pretreated with RUCM cells) was significantly reduced (Fig. 4, $p < .001$), being only 31.9% ± 2.2% and 24.9% ± 2.6% in the left and right CA1 regions, respectively. Seven days after resuscitation, one of the seven animals in group D was nonresponsive to pain stimulation in the tail.

The percentages of the damaged pyramidal neurons in the left and right CA1 regions of the dorsal hippocampus in the four experimental groups are summarized in Figure 4. For groups A (sham group), B (untreated CA), and C (CA pretreated with DM), the injuries are symmetrical, and there is no significant difference between left and right hemispheres. In group D (CA pretreated with RUCM cells), although both sides had significantly less injury compared with groups B (untreated) and C (pretreated with DM) ($p < .001$), the side with microinjection had slightly more damage than the contralateral side ($p = .0496$).

The transplanted RUCM cells were identified by the loaded green CFDA dye under a fluorescent microscope. It is evident that the transplanted RUCM cells have survived after the microinjection (Fig. 5). A significant amount of RUCM cells have migrated away from the injection sites. Figure 6 shows the 3D rendering of the migration of CFDA-labeled RUCM cells from the injection sites. Unlike in focal cerebral ischemia, the neuronal damage in global cerebral ischemia is not localized. There seems no clear direction for RUCM cell migration after ischemia, and migration patterns vary from rat to rat. In some rats, a majority of the cells injected into the cortex migrated toward the CC, and those injected directly into the CC migrated the furthest medially toward the contralateral side. In other rats, cells injected in the dorsal hippocampus showed migrations in the medial-lateral and rostral-caudal directions. Cells transplanted in DTN had shorter migration distances. Only a few RUCM cells were found directly in the CA1 regions of the transplantation side, and no CFDA-labeled RUCM cells were found on the contralateral side.

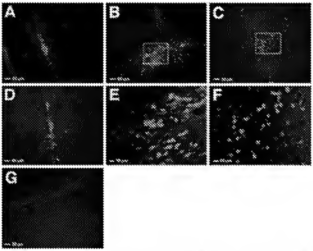

Figure 5. Representative fluorescence images of carboxyfluorescein diacetate-dyed rat umbilical cord matrix cells transplanted 3 days prior to cardiac arrest into the rat brains. Brains were sectioned 7 days after the cardiac arrest and resuscitation. The transplanted cells were found to have survived and migrated away from the injection sites in (**A**) cortex, (**B**) corpus callosum, (**C**) dorsal hippocampus, and (**D**) dorsal thalamic nucleus (×100 magnification). The areas within the white rectangles in (**B**) and (**C**) are further magnified at ×400 to show details of the transplanted cells in (**E**) corpus callosum and (**F**) dorsal hippocampus, respectively. A section from a medium-injected rat is provided in (**G**), showing the level of background autofluorescence for comparison.

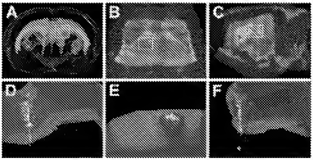

Figure 6. Three-dimensional reconstruction of the migration of the transplanted carboxyfluorescein diacetate (CFDA)-labeled rat umbilical cord matrix stem cells in the brain of a rat 10 days after the cell transplantation and 7 days after cardiac arrest and resuscitation. Images show (**A**) the front view in the rostral-to-caudal direction, (**B**) top view in the dorsal-to-ventral direction, and (**C**) left-side view in the lateral-to-medial direction. Images (**D**), (**E**), and (**F**) depict the zoom-in views of the regions enclosed in the white boxes in (**A**), (**B**), and (**C**), respectively. Anatomic references are color-coded: magenta, outline of the brain; cyan, corpus callosum; purple, hippocampus; and red, ventricles. The green spheres mark the injection sites, and the yellow spheres are outlines of the CFDA-labeled rat umbilical cord matrix stem cells.

Discussion

One of the characteristics of brain damage caused by cerebral global ischemia after CA is the disseminated neuronal loss, particularly in the selectively vulnerable CA1, CA3, and dentate gyrus regions of hippocampus. Often the dying or dead neurons are found side-by-side to "good" neurons that appear histologically normal. The underlying molecular and cellular events determining the fate of each neuron after the same ischemic insult are not fully understood.

Using a highly reproducible outcome model of CA and resuscitation, we demonstrated the potential therapeutic effects of transplanted UCM cells on mitigating neuronal loss after severe global ischemia. We found that pretreatment with RUCM cells 3 days before CA can significantly reduce, but not eliminate, brain damage characterized by the pyramidal neuron loss in the CA1 region of the hippocampus. As shown in Figures 3 and 4, the group pretreated with RUCM cells (group D) had significantly less CA1 damage than the untreated group (group B). Possible artifacts unrelated to the direct therapeutic effects of RUCM cells include immune response to microinjection and brain preconditioning to ischemia due to microinjection procedures. However, others [40] have shown that injection of porcine UCM cells into rat brain do not elicit immune response. In this study, we further ruled out any possible preconditioning artifacts by adding group C (pretreated with defined medium), in which the exact same pretreatment procedures were performed as in group D except for receiving RUCM cells. Group C showed no improvement in histology outcome due to preconditioning alone. In fact, microinjection with sterilized DM followed by CA 3 days later had the tendency to slightly worsen the outcome compared with untreated group (group B), and the difference between groups B (untreated) and C (pretreated with DM only) was statistically significant on the injection side. Thus, it can be concluded that the observed improvement in histological outcome in group D was a direct consequence of RUCM cell treatment.

The general assumption about stem cells being beneficial in treating a stroke is their pluripotency. In embryonic stem cells, pluripotency has been linked to the expression of Oct-4, a Pit-Oct-Unc transcription factor [41]. Oct-4 is expressed almost exclusively in embryonic stem cells [42]. In the mature animal, Oct-4 expression was thought to be restricted to the germline. However, Oct-4 expression was recently observed in a population of bone marrow stromal cells after serum deprivation [43] and porcine UCM cells [44]. Oct-4 expression has also been found in amniotic fluid cells [45] and in tumors [46, 47]. Although pluripotency and functionality in these latter cases are yet to be established, these findings nevertheless suggest that Oct-4 might play a role in determining the fate of other types of stem cells.

The Oct-4$^+$ cells used in this study were derived from the RUCM. These cells have the potential to differentiate into other tissue types. For example, it was demonstrated that human UCM cells had the capacity to differentiate into a neuronal phenotype in vitro [36] and that porcine UCM cells not only could survive after transplantation into the rat brain, but also appeared to differentiate into neurons [40]. We showed here that RUCM cells are myofibroblast-like stem cells similar to those isolated from porcine and human umbilical cord. They express markers similar to those found in the adult bone marrow stromal stem cell (SMA and vimentin) and embryonic stem cells (Oct-4). These findings suggest that the UCM is an abundant, easily obtainable source of primitive Oct-4$^+$ stem cells that might be intermediate between embryonic and adult stem cells. Unlike embryonic stem cells, UCM cells do not form teratomas (K. Mitchell, unpublished observations) nor do they elicit a detectable immune response [40, 48]. The UCM cells might in fact have an immune-suppressive effect as has been observed for mesenchymal stem cells [49]. Mesenchymal stem cells from cord blood, while having many of the same characteristics as the UCM cells, are less abundant and might be less primitive than those found in UCM. Because of these properties, UCM cells might be a better alternative to embryonic, bone marrow stromal, or umbilical cord blood cells for cell-based therapies.

We chose a pretreatment strategy in this study to evaluate the possible mode of action of stem cells in preventing neuronal damage after an intrinsically disseminated insult. Our rationale was that with pretreatment, the transplanted stem cells could be activated by the acute exposure to ischemia. If pretreatment can significantly improve the histological outcome after a controlled global ischemia, which is known to lead to nonfocal damages, then neither of the two popular hypotheses about stem cell protection (namely, stem cell differentiation into neurons [transdifferentiation] and stem cell fusion with host cells) would be sufficient to explain the protective effects. Other mechanisms should be considered and explored.

Indeed, careful analysis of the engraftment and migration of the transplanted cells suggests that RUCM cell transdifferentiation and fusion might not be the predominant mechanisms for the observed protection. Although significant cell migration within hippocampus was observed in some of the animals (Fig. 6), relatively few RUCM cells were found directly in the CA1 pyramidal cell lining on the transplantation side, and no fluorescent cells were detectable on the contralateral side. Thus, even if RUCM cell transdifferentiation into neurons or RUCM cell fusion with neuronal cells does occur during the reperfusion and recovery period, neither mechanism can account for the significant protection seen in group D (pretreated with RUCM cells). Hence, our results seem to suggest the possibility of a third novel mechanism of stem cell repair—one that elicits one or multiple synergistic extracellular signaling pathways. This possibility is strongly supported by the recent studies in which i.v. injection of human umbilical cord blood (HUCB) cells into rats was shown to reduce brain injury during a 1-hour middle cerebral artery occlusion [50, 51]. These focal ischemia studies unequivocally demonstrated that cell entry into the central nervous system is not absolutely required for the neuroprotection by the peripherally injected HUCB cells. As the authors of these studies concluded, the secretion of the "therapeutic molecules" (including the neurotrophic factors) and the nonimmune anti-inflammatory effects are the two necessary components of the observed HUCB cell neuroprotection.

In our case, it can be speculated that the presence of Oct-4$^+$ RUCM cells during ischemia activates and accelerates the proliferation and recruitment of the endogenous neuronal stem cells, including re-entry of quiescent stem cells, into the rescue effort. Other possibilities include the creation of an extracellular milieu that enhances and restores the intrinsic ability of the brain tissue in self-repair [52]. For example, it is possible that the very presence of the transplanted stem cells serves as the first responder to the stress signals from ischemia, priming the activation and reintegration of the Notch and Wnt signaling [53] to renew the adult brain tissue to re-enter a youthful state [54, 55] in the recovery stage. After the initial increase in the proliferation of endogenous neuronal progenitor cells, asymmetric antagonization of Notch signal can lead to rapid differentiation of one of the two daughter cells into vascular lineage for angiogenesis or neuronal lineage for neurogenesis. Another possibility is that, like the cord blood cells, the transplanted RUCM cells can suppress the inflammatory response after ischemia [56], thereby helping injured neurons to recover and promoting the viable neurons to remain alive. The transplanted-cell-host-cell communication as the primary stem cell repair mechanism is further suggested in our study by the improved outcome in the contralateral side where no transplanted RUCM cells were found—a strong indication that retrograde signaling from long-distance connections might also play an important role in determining the fate of neurons after ischemia and reperfusion injuries.

Although the most desirable intervention for cerebral ischemia is post-treatment, preventative therapy by pretreatment to avoid brain damage due to circulatory arrest is also clinically relevant. For example, patients receiving an implantable automatic internal cardiac defibrillator usually undergo two tests of total cerebral ischemia. Also, in pediatric cardiac surgery for repairing complex congenital cardiac malformations [57], in certain adult cardiac surgeries involving the aortic arch [58, 59], and in adult neurosurgery for giant intracranial aneurysms [60, 61], a controlled total circulatory arrest to create a bloodless operative field is often essential. At present, the only commonly used preventative measure in these surgical cases is deep hypothermia, which is not without devastating complications. Thus, devising novel pretreatment strategies aimed at alleviating acute and delayed neurological morbidities is highly beneficial to the future development of innovative medical procedures. Most importantly, the potential future clinical applications of stem cell therapy require a better understanding of the protection mechanisms, for which pretreatment clearly has the advantage over post-treatment in many cases, as discussed above.

Finally, it is worth mentioning that, although we have attempted to use clonal cells for transplantation, it is difficult to conclude that the endothelial cells from the umbilical cord tissue are completely depleted after multiple passages. However, endothelial and vascular cells do not express Oct-4 nor would they proliferate as long in culture as the UCM cells. There is a remote possibility that a very small fraction (<1%) of the injected cells might be endothelial precursors, which might have persisted in culture over multiple passages. Based on the percentage of cells that are positive for SMA and Oct-4 (markers that would not be expressed by endothelial precursors), the very small percentage of endothelial precursors, if any, would be unlikely to contribute substantially to the overall effect observed.

Conclusion

RUCM cell transplantation indirectly reduces the percentage of damaged hippocampal neurons after CA. Although more studies will be needed to ascertain the protection mechanism, the results of the present study indicate that Oct-4$^+$ UCM cell treatment of brain injury from global ischemia, particularly through cell signaling pathways, is a distinct possibility and warrants further investigation. A better understanding of the extracellular signaling molecules that are secreted by UCM cells in different environments (e.g., hypoxia) can also help identify potential targets for the development of novel drugs that—when given *after* CA—can potentially trigger the same healing process that the UCM cells appear to have initiated.

Acknowledgments

We thank Katayoun Ghajarnia for participating in histology tissue preparation and neuronal counting and Deanna Nachreiner for help with histology analysis and 3D rendering of stem cell migration. This work was supported by a grant from the National Institutes of Health (R01NS/HL036124 to Y.X.) and was presented at the November 12–16, 2005 Society for Neuroscience annual meeting.

Disclosures

The authors indicate no potential conflicts of interest.

References

1 Liachenko S, Tang P, Hamilton RL et al. Regional dependence of cerebral reperfusion after circulatory arrest in rats. J Cereb Blood Flow Metab 2001;21:1320–1329.
2 Liachenko S, Tang P, Hamilton RL et al. A reproducible model of circulatory arrest and remote resuscitation in rats for NMR investigation. Stroke 1998;29:1229–1238; discussion 1238–1229.
3 Xu Y, Liachenko S, Tang P. Dependence of early cerebral reperfusion and long-term outcome on resuscitation efficiency after cardiac arrest in rats. Stroke 2002;33:837–843.
4 Bhardwaj A, Alkayed NJ, Kirsch JR et al. Mechanisms of ischemic brain damage. Curr Cardiol Rep 2003;5:160–167.
5 Hossmann KA. Reperfusion of the brain after global ischemia: Hemodynamic disturbances. Shock 1997;8:95–101; discussion 102–103.
6 Yushmanov VE, Wang L, Liachenko S et al. ADC characterization of region-specific response to cerebral perfusion deficit in rats by MRI at 9.4 T. Magn Reson Med 2002;47:562–570.
7 Wang L, Yushmanov VE, Liachenko SM et al. Late reversal of cerebral perfusion and water diffusion after transient focal ischemia in rats. J Cereb Blood Flow Metab 2002;22:253–261.
8 Liachenko S, Tang P, Xu Y. Deferoxamine improves early postresuscitation reperfusion after prolonged cardiac arrest in rats. J Cereb Blood Flow Metab 2003;23:574–581.
9 Chauhan N, Zhao Z, Barber PA et al. Lessons in experimental ischemia for clinical stroke medicine. Curr Opin Neurol 2003;16:65–71.
10 Green AR, Ashwood T. Free radical trapping as a therapeutic approach to neuroprotection in stroke: Experimental and clinical studies with NXY-059 and free radical scavengers. Curr Drug Targets CNS Neurol Disord 2005;4:109–118.
11 Ren JM, Finklestein SP. Growth factor treatment of stroke. Curr Drug Targets CNS Neurol Disord 2005;4:121–125.
12 Kokaia Z, Lindvall O. Neurogenesis after ischaemic brain insults. Curr Opin Neurobiol 2003;13:127–132.
13 Kuhn HG, Dickinson-Anson H, Gage FH. Neurogenesis in the dentate gyrus of the adult rat: Age-related decrease of neuronal progenitor proliferation. J Neurosci 1996;16:2027–2033.
14 Takagi Y, Nozaki K, Takahashi J et al. Proliferation of neuronal precursor cells in the dentate gyrus is accelerated after transient forebrain ischemia in mice. Brain Res 1999;831:283–287.
15 Liu J, Solway K, Messing RO et al. Increased neurogenesis in the dentate gyrus after transient global ischemia in gerbils. J Neurosci 1998;18:7768–7778.
16 Kee NJ, Preston E, Wojtowicz JM. Enhanced neurogenesis after transient global ischemia in the dentate gyrus of the rat. Exp Brain Res 2001;136:313–320.
17 Nakatomi H, Kuriu T, Okabe S et al. Regeneration of hippocampal pyramidal neurons after ischemic brain injury by recruitment of endogenous neural progenitors. Cell 2002;110:429–441.
18 Pencea V, Bingaman KD, Wiegand SJ et al. Infusion of brain-derived neurotrophic factor into the lateral ventricle of the adult rat leads to new neurons in the parenchyma of the striatum, septum, thalamus, and hypothalamus. J Neurosci 2001;21:6706–6717.
19 Larsson E, Mandel RJ, Klein RL et al. Suppression of insult-induced neurogenesis in adult rat brain by brain-derived neurotrophic factor. Exp Neurol 2002;177:1–8.
20 Popp E, Padosch SA, Vogel P et al. Effects of intracerebroventricular application of brain-derived neurotrophic factor on cerebral recovery after cardiac arrest in rats. Crit Care Med 2004;32(suppl 9):S359–S365.
21 Yoshimura S, Takagi Y, Harada J et al. FGF-2 regulation of neurogenesis in adult hippocampus after brain injury. Proc Natl Acad Sci U S A 2001;98:5874–5879.
22 Shingo T, Sorokan ST, Shimazaki T et al. Erythropoietin regulates the in vitro and in vivo production of neuronal progenitors by mammalian forebrain neural stem cells. J Neurosci 2001;21:9733–9743.
23 Savitz SI, Dinsmore JH, Wechsler LR et al. Cell therapy for stroke. NeuroRx 2004;1:406–414.
24 Li Y, Chen J, Chen XG et al. Human marrow stromal cell therapy for stroke in rat: Neurotrophins and functional recovery. Neurology 2002;59:514–523.
25 Chen J, Li Y, Wang L et al. Therapeutic benefit of intravenous administration of bone marrow stromal cells after cerebral ischemia in rats. Stroke 2001;32:1005–1011.
26 Honma T, Honmou O, Iihoshi S et al. Intravenous infusion of immortalized human mesenchymal stem cells protects against injury in a cerebral ischemia model in adult rat. Exp Neurol 2006;199:56–66.
27 Veizovic T, Beech JS, Stroemer RP et al. Resolution of stroke deficits following contralateral grafts of conditionally immortal neuroepithelial stem cells. Stroke 2001;32:1012–1019.
28 Kelly S, Bliss TM, Shah AK et al. Transplanted human fetal neural stem cells survive, migrate, and differentiate in ischemic rat cerebral cortex. Proc Natl Acad Sci U S A 2004;101:11839–11844.
29 Chen J, Sanberg PR, Li Y et al. Intravenous administration of human umbilical cord blood reduces behavioral deficits after stroke in rats. Stroke 2001;32:2682–2688.
30 Sanberg PR, Willing AE, Garbuzova-Davis S et al. Umbilical cord blood-derived stem cells and brain repair. Ann N Y Acad Sci 2005;1049:67–83.
31 Direkze NC, Forbes SJ, Brittan M et al. Multiple organ engraftment by bone-marrow-derived myofibroblasts and fibroblasts in bone-marrow-transplanted mice. STEM CELLS 2003;21:514–520.
32 Harris RG, Herzog EL, Bruscia EM et al. Lack of a fusion requirement for development of bone marrow-derived epithelia. Science 2004;305:90–93.
33 Hashimoto N, Jin H, Liu T et al. Bone marrow-derived progenitor cells in pulmonary fibrosis. J Clin Invest 2004;113:243–252.
34 Forbes SJ, Russo FP, Rey V et al. A significant proportion of myofibroblasts are of bone marrow origin in human liver fibrosis. Gastroenterology 2004;126:955–963.
35 Jin K, Mao XO, Sun Y et al. Stem cell factor stimulates neurogenesis in vitro and in vivo. J Clin Invest 2002;110:311–319.
36 Mitchell KE, Weiss ML, Mitchell BM et al. Matrix cells from Wharton's jelly form neurons and glia. STEM CELLS 2003;21:50–60.
37 Paxinos G, Watson C. The Rat Brain in Stereotaxic Coordinates. 4th ed. San Diego, CA: Academic Press, 1998.
38 Neumar RW, Bircher NG, Sim KM et al. Epinephrine and sodium bicarbonate during CPR following asphyxial cardiac arrest in rats. Resuscitation 1995;29:249–263.
39 Fiala JC. Reconstruct: A free editor for serial section microscopy. J Microsc 2005;218:52–61.
40 Weiss ML, Mitchell KE, Hix JE et al. Transplantation of porcine umbilical cord matrix cells into the rat brain. Exp Neurol 2003;182:288–299.
41 Suzuki N, Rohdewohld H, Neuman T et al. Oct-6: A POU transcription factor expressed in embryonal stem cells and in the developing brain. Embo J 1990;9:3723–3732.
42 Pesce M, Schöler HR. Oct-4: Control of totipotency and germline determination. Mol Reprod Dev 2000;55:452–457.
43 Pochampally RR, Smith JR, Ylostalo J et al. Serum deprivation of human marrow stromal cells (hMSCs) selects for a subpopulation of early progenitor cells with enhanced expression of OCT-4 and other embryonic genes. Blood 2004;103:1647–1652.
44 Carlin R, Davis D, Weiss M et al. Expression of early transcription factors Oct4, Sox2 and Nanog by porcine umbilical cord (PUC) matrix cells. Reprod Biol Endocrinol 2006;4:8.
45 Prusa AR, Marton E, Rosner M et al. Oct-4-expressing cells in human amniotic fluid: A new source for stem cell research? Hum Reprod 2003;18:1489–1493.
46 Gidekel S, Pizov G, Bergman Y et al. Oct-3/4 is a dose-dependent oncogenic fate determinant. Cancer Cell 2003;4:361–370.
47 Monk M, Holding C. Human embryonic genes re-expressed in cancer cells. Oncogene 2001;20:8085–8091.
48 Medicetty S, Bledsoe AR, Fahrenholtz CB et al. Transplantation of pig stem cells into rat brain: Proliferation during the first 8 weeks. Exp Neurol 2004;190:32–41.
49 Aggarwal S, Pittenger MF. Human mesenchymal stem cells modulate allogeneic immune cell responses. Blood 2005;105:1815–1822.
50 Borlongan CV, Hadman M, Sanberg CD et al. Central nervous system entry of peripherally injected umbilical cord blood cells is not required for neuroprotection in stroke. Stroke 2004;35:2385–2389.
51 Vendrame M, Gemma C, de Mesquita D et al. Anti-inflammatory effects of human cord blood cells in a rat model of stroke. Stem Cells Dev 2005;14:595–604.
52 Prockop DJ, Gregory CA, Spees JL. One strategy for cell and gene therapy: Harnessing the power of adult stem cells to repair tissues. Proc Natl Acad Sci U S A 2003;100(suppl 1):11917–11923.
53 Duncan AW, Rattis FM, DiMascio LN et al. Integration of notch and wnt signaling in hematopoietic stem cell maintenance. Nat Immunol 2005;6:314–322.
54 Conboy IM, Conboy MJ, Wagers AJ et al. Rejuvenation of aged progenitor cells by exposure to a young systemic environment. Nature 2005;433:760–764.
55 Conboy IM, Rando TA. Aging, stem cells and tissue regeneration: Lessons from muscle. Cell Cycle 2005;4:407–410.
56 Garbuzova-Davis S, Willing AE, Desjarlais T et al. Transplantation of human umbilical cord blood cells benefits an animal model of Sanfilippo syndrome type B. Stem Cells Dev 2005;14:384–394.
57 Amir G, Ramamoorthy C, Riemer RK et al. Neonatal brain protection and deep hypothermic circulatory arrest: Pathophysiology of ischemic neuronal injury and protective strategies. Ann Thorac Surg 2005;80:1955–1964.

58 Augoustides JG, Pochettino A, Ochroch EA et al. Clinical predictors for prolonged intensive care unit stay in adults undergoing thoracic aortic surgery requiring deep hypothermic circulatory arrest. J Cardiothorac Vasc Anesth 2006;20:8–13.
59 Kieradi T, Rausi SS, Nissen NN et al. Cavo-atrial tumor resection under total circulatory arrest without a sternotomy. Ann Thorac Surg 2006;81:1887–1888.
60 Strebel S, Mendelowitsch A, Kindler C. Rupture of a giant intracranial aneurysm while starting cardiopulmonary bypass for hypothermic circulatory arrest. J Neurosurg Anesthesiol 2004;16:263–265.
61 Young WL, Lawton MT, Gupta DK et al. Anesthetic management of deep hypothermic circulatory arrest for cerebral aneurysm clipping. Anesthesiology 2002;96:497–503.

Potential Treatment of Cerebral Global Ischemia with Oct-4+ Umbilical Cord Matrix Cells

Sachiko Jomura, Marc Uy, Kathy Mitchell, Renee Dallasen, Claudia J. Bode and Yan Xu

Stem Cells 2007;25;98-106; originally published online Sep 7, 2006;
DOI: 10.1634/stemcells.2006-0055

TAB 3

Job: Lester (307-2)
Chapter: 03/Mitchell
Pub Date:
Template: CE/6x9 Template/Rev.04.03

Operator: SV
Date: 9/04
Revision: 1st Pass

3 Umbilical Cord Stem Cells

Kathy E. Mitchell

CONTENTS

1. INTRODUCTION

The two most basic properties of stem cells are the capacities to self-renew and to differentiate into multiple cell or tissue types *(1–3)*. Generally, stem cells are categorized as one of three types: embryonic stem cells (ES), embryonic germ cells (EG), or adult stem cells. ES cells are derived from the inner cell mass of Q1 the blastula (Fig. 1). They proliferate indefinitely and can differentiate spontaneously into all three tissue layers of the embryo *(4)* and into germ cells as well *(5–7)*. EG cells are derived from primordial germ cells (*see* Fig. 1), a small set of stem cells that reside in the protected environment of the yolk stalk, so that they remain undifferentiated during embryogenesis. As with ES cells, EG cells have the capacity to differentiate into all three tissue layers *(8)*. Adult stem cells are found in most tissues and in the circulation. They may have less replicative capacity than ES or EG cells and, until recently, were thought to have restricted developmental fates *(9)*. This classification system omits a significant source of stem cells derived from the extraembryonic tissues (umbilical cord, placenta and amniotic tissues/fluids), which are derived from neither the adult organism nor the embryo proper. This review will describe studies of stem cells derived from

From: *Contemporary Endocrinology: Stem Cells in Endocrinology*
Edited by L. B. Lester © Humana Press Inc., Totowa, NJ

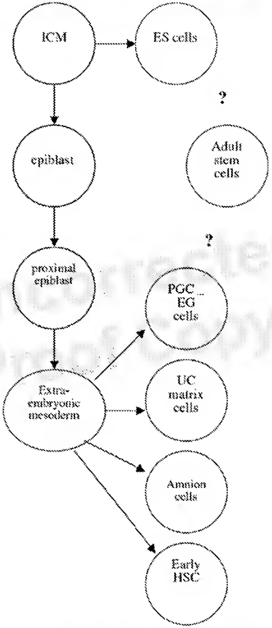

Fig. 1. Stem cells and origins from inner cell mass (ICM) and extraembryonic mesoderm. ES cells arise from cells derived from the ICM. EG cells, umbilical cord matrix cells, cells from amniotic tissues, and early hematopoietic stem cells (HSC) arise from extraembryonic mesoderm.

Job: Lester (407-2)
Chapter: 03/Mitchell
Pub Date:
Template: CE/6x9/Template/Rev.04/03
Operator: SV
Date: 9/04
Revision: 1st Pass

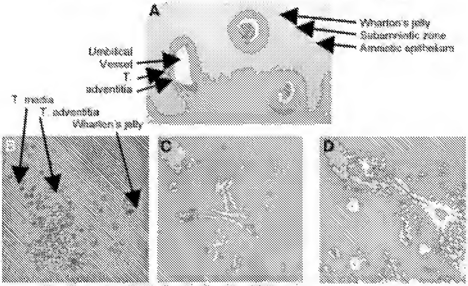

Fig. 2. Human umbilical cord matrix cells. **(A)** Umbilical cords have two arteries and one vein surrounded by Wharton's jelly. **(B)** Pockets of cobblestone-appearing cells between the adventitia and Wharton's jelly. **(C)** Umbilical cord matrix cells in culture. **(D)** Human umbilical cord cells treated by neural induction method of Woodbury et al. *(33)*.

extraembryonic tissues with an emphasis on cells derived from umbilical cord, their developmental origins, and relationships to other types of stem cells and potential in regenerative medicine.

2. STRUCTURE AND DEVELOPMENT OF THE UMBILICAL CORD

The fully developed umbilical cord has one vein and two arteries surrounded by mucous or gelatinous connective tissue also known as Wharton's jelly and is covered with amnion (Fig. 2). There are three distinct zones of stromal cells and matrix that can be identified: subamniotic layer, Wharton's jelly, and media and adventitia surrounding the vessels but no differences along the longitudinal axis *(10)*. The Wharton's jelly region, the most abundant, has cleft-like spaces of stroma matrix molecules of collagens type I, III, and VI, with collagen type VI, laminin, and heparin sulphate proteoglycan around the clefts. The jelly-filled, cleft-like spaces are surrounded by stromal cells that are slender and spindle-shaped myofibroblasts that express vimentin and smooth muscle actin as well as

Job: Lester (487-2)
Chapter: 03/Mitchell
Pub Date:
Template: CE/6x9/Template/Rev.04.03

Operator: SV
Date: 9/04
Revision: 1st Pass

desmin *(11)*. Earlier cords have only vimentin and desmin. The structure and composition of the umbilical cord, rich in highly resilient matrix and myofibroblasts, protects the vessels from compression and may also facilitate an exchange between cord blood and amniotic fluid.

The umbilical cord is derived from extraembryonic mesoderm (*see* Fig. 1). After the blastula develops, cells from the inner cell mass (from which ES cells are derived) form the epiblast *(12)*. Cells destined to become the extraembryonic mesoderm arise from the proximal epiblast and are the earliest mesoderm to migrate through the primitive streak *(13)*. Extraembryonic mesoderm increases over the next few stages of embryogenesis to line the trophectoderm shell, the amniotic ectoderm, and the yolk sac endoderm and form the connecting stalk as well. Thus extraembryonic mesoderm contributes to the chorion, amnion, yolk sac, and, eventually, the umbilical cord *(14)*.

Primordial germ cells (from which EG stem cells are derived) and early hematopoietic stem cells arise from extraembryonic mesoderm (*see* Fig. 1). Hematopoiesis occurs in the yolk sac blood islands 8–8.5 days postconception in the mouse *(15, 16)*. These yolk sac hematopoietic stem cells provide early, local hematopoiesis during development and circulate through the embryo to provide oxygen and nutrients. Primordial germ cells arise from the extraembryonic mesoderm and appear in the yolk sac as distinguishable entities at about 7 days postconception in the mouse *(17)*. They migrate to the genital ridges of the developing fetus by about 11.5–12.5 days postconception. Primordial germ cells retrieved from the genital ridges and cultured in vitro are multipotential *(8)*. The migration of primordial germ cells is controlled by a number of factors, including c-Kit and members of the nanos family *(18)*. Primordial germ cells, which do not home correctly to the genital ridges, undergo apoptosis. If apoptosis does not occur, these cells can form pediatric germ cell tumors *(19)*.

Recent work has shown that the umbilical cord is a rich source of stem cells. Ende coined the term *Berashis cells*, meaning beginning cells, to describe the primitive multipotential cells found in human umbilical cord blood and suggested that they may be related to fetal stem cells *(20, 21)*. Three types of stem cells have been identified in umbilical cord: myofibroblast-like cells from the umbilical cord matrix, and hematopoietic and mesenchymal stem cells from cord blood. Stem cells obtained from umbilical cord and placental blood express low levels of human leukocyte antigens (HLA) and have a universal donor potential *(22)*. This is an important source of stem cells for bone marrow replacement when HLA-matched donors cannot be found. The properties of umbilical cord stem cells, their relationship to other types of stem cells, and their immunogenic properties are areas of much interest in the emerging fields of stem cell biology and regenerative medicine.

Au: HLA correct as spelled out?

Job: Lester (387-7)
Chapter: 03/Mitchell
Pub Date:
Template: CE/6x9/Template/Rev.04.03

Operator: SV
Date: 9/04
Revision: 1st Pass

3. STEM CELLS DERIVED FROM EXTRAEMBRYONIC TISSUES

3.1. Umbilical Cord Matrix Cells

Umbilical cord matrix may be the remnants of the yolk stalk, the protected environment where early hematopoietic stem cells and primordial germ cells arise. As such, it may be a reservoir of cells with stem cell–like characteristics that can migrate into the developing fetus at appropriate times during development. Umbilical cord matrix cells express markers for stem cells, including many that are expressed in ES, EG, and neural precursor or stem cells (Table 1). In addition, umbilical cord matrix cells can be easily expanded and maintained in culture for more than 80 population doublings. They express low levels of telomerase. They also form structures reminiscent of embryoid bodies when cultured past confluence. They express smooth muscle actin and vimentin, markers for myofibroblasts; nestin, neuron-specific enolase (NSE), and glial fibrillary acidic protein (GFAP), markers for neural stem cells; and c-Kit, Oct-4, Tra-1-60, markers expressed in ES and EG cells. Importantly, umbilical cord matrix cells do not form teratomas in nude mice *(23)* or when injected into rat brain or muscle *(24)*.

Pluripotency of ES cells has been linked to expression of Oct-4, a Pit-Oct-Unc transcription factor *(25)*. Until recently, it was believed that Oct-4 expression in mature animals was confined exclusively to germ cells *(26)*. Initially expressed in all cells in the blastula, Oct-4 becomes restricted to the inner cell mass at the blastula stage. Oct-4 is expressed by nearly 100% of isolated umbilical cord matrix cells after 10 passages and is localized to the nucleus. The full-length transcript was cloned from umbilical cord matrix cells and has 100% homology to the reported human embryonic form of Oct-4 *(23)*. The role of Oct-4 in umbilical cord matrix cells is not known. In ES cells, the precise level of Oct-4 expression seems to determine cell fate with high levels of Oct-4 expression pushing ES cells toward extraembryonic mesoderm or endodermal lineages and low Oct-4 expression resulting in cells that become trophectoderm *(27)*. Only ES cells expressing normal Oct-4 levels remained pluripotent. Recently, a population of bone marrow stromal cells was isolated after serum deprivation that expressed Oct-4 *(28)*. Oct-4 expression was also found in amniotic fluid cells *(29)*. Taken together, these findings suggest that Oct-4 may play a role in nonembryonic stem cells. This is being investigating for umbilical cord matrix cells in our laboratory.

Umbilical cord matrix cell express many of the markers Shamblott et al. *(30)* identified in derivatives of cultured EG cells including NSE, vimentin, and nestin—markers for neural precursors,—and glial markers, 2',3'-cyclic nucleotide 3'-phosphodiesterase, and GFAP, also expressed in early neural precursors (*see* Table 1). In addition, umbilical cord matrix cells express c-Kit, which is

Job: Lester (487-2)
Chapter: 03/Mitchell
Pub Date:
Template: CE/6x9/Template/Rev.04.03

Operator: SV
Date: 9/04
Revision: 1st Pass

Table 1
Comparison of Markers for Stem Cells Expressed in ES, EG, UCM, Amniotic, and NS Cells

	ES cells	*EG cells*	*UCM cells*	*Amniotic*	*NS cells*
Oct-4	+	+	+	+	NA
Telomerase	+	+	+	+	–
Vimentin	NA	+	+	+	+
Nestin	NA	+	+	+	+
NSE	NA	+	+	+	+
GFAP	NA	+	+	+	+

ES, embronic stem; EG, embryonic germ; UCM, umbilical cord matrix; NS, neural stem; NSE, neuron-specific enolase; GFAP, glial fibrillary acidic protein; NA, not applicable.

important for proper migration of primordial germ cells. Expression of these proteins, including Oct-4, by both umbilical cord matrix cells and EG cells suggests a possible relationship between the two cell types, particularly in light of their residing in the same region of the developing fetus and common origin from extraembryonic mesoderm.

Umbilical cord matrix cells can be differentiated to form neuron-like cells based on morphology, expression of neuron-specific proteins, and development of voltage-gated potassium channels found in early neurons that are important for development of electrical excitability *(31, 32)*. Some cells differentiate spontaneously to express neuronal markers. Induction by the method of Woodbury et al. *(33)* greatly enhances the number of cells that differentiate into a neuron-like cell (approximately 80%) *(31)*. Umbilical cord matrix cells induced by this method form primitive networks between the cells with long axon-like processes, refractile cell bodies and dendrite-like processes, highly reminiscent of primary neurons in culture (Fig. 2D). The induced umbilical cord matrix cells express neurofilament M, Tuj1, growth cone–associated protein (GAP43), and tyrosine hydroxylase, which are markers for more mature neurons. Thus, as with many stem cells, umbilical cord matrix stem cells appear to differentiate along a neuronal fate readily, with some differentiation occurring spontaneously.

Umbilical cord matrix cells have also been used in in vivo xenotransplantation. Studies by Weiss et al. *(24)* suggest that porcine umbilical cord matrix cells survive, migrate, and begin to express markers for mature neurons when transplanted into rat brain. Umbilical cord matrix cells loaded with the fluorescent dye, PKH26, were transplanted into rat brains and detectable at periods from 2 to 6 weeks after transplantation. After 4 weeks, the umbilical cord matrix cells were detected primarily along the injection tract and were small and spherical,

Job: Lester (307-2)
Chapter: 03/Mitchell
Pub Date:
Template: CE/6x9/Template/Rev.#4.03

Operator: SV
Date: 9/04
Revision: 1st Pass

with very few processes. However, the transplanted umbilical cord cells did express neuronal filament 70 (NF70) based on detection with an antibody specific for porcine but not rodent NF70. In contrast, 6 weeks after injection, about 10% of the detectable umbilical cord matrix cells had migrated away from the injection site and into the region just ventral to the corpus callosum. These umbilical cord matrix cells also expressed NF70. Taken together, these studies suggest that umbilical cord matrix cells may have the capacity to differentiate into neurons in vitro and in vivo. More work needs to be done to establish that the umbilical cord matrix cells can generate action potentials in vitro and form new neuronal connections in vivo. Studies are under way to address these issues and to establish whether umbilical cord matrix cells can ameliorate neural deficits after oxygen deprivation of the brain or in a Parkinson's disease model in rat.

3.2. Umbilical Cord Blood Cells

Umbilical cord blood is a rich source of hematopoietic stem/progenitor cells and has been used successfully as an important source of cells for hematopoietic stem cell (HSC) transplantation *(34)*. Although somewhat controversial, umbilical cord blood is also thought to be a source of mesenchymal stem cells (MSC). MSC can be differentiated into cells other than blood, but may also be important for long-term engraftment in bone marrow transplants with umbilical cord blood *(35)*. There is much interest in the potential of umbilical cord blood as a source of multipotential stem cells; umbilical cord blood is often banked and cryogenically stored for use by the individual from whom the cord blood was taken or as a source for donation to other individuals in need of bone marrow transplants or other cell-based therapies.

Umbilical cord blood is an important source of HSC for bone marrow transplants for which HLA-matched donors cannot be found. Umbilical cord blood stem cell progenitors are used now routinely as an alternative to bone marrow transplant *(36)*. There are many potential advantages in using the HSC from cord blood as compared with HSC derived from bone marrow. First, HSC in umbilical cord blood occur at higher frequency than in peripheral blood *(37)* and at comparable levels to their occurrence in bone marrow, making up about 2% of the total mononuclear cell population *(38)*. Importantly, umbilical cord HSC have a greater ability to replicate than bone marrow-derived HSC and can be manipulated genetically as well *(39)*. They can be collected noninvasively with no risk to mother or child. Because of their increased proliferative rate, HSC can be expanded ex vivo, unlike adult hematopoietic stem cells *(40, 41)*. This potential for expansion can be augmented by treatment with a cocktail of growth factors (TPO, SCF, interleukin-3, FL, and basic fibroblastic growth factor) allowing for a 500-fold expansion of $CD34^+$ HSC from umbilical cord blood *(42)*. $CD34^+$

Au: Please spell out TPO, SCF, FL. Also, is IL spelled out correctly?

Job: Lester (487-3)
Chapter: 03/Mitchell
Pub Date:
Template: CE/6x9/Template/Rev.04.03
Operator: SV
Date: 9/04
Revision: 1st Pass

umbilical cord cells may also have potentials beyond the hematopoietic lineages. Pesce et al. *(43)* showed that CD34⁺ umbilical cord cells can differentiate into muscle fibers in immune-suppressed mice and can also form myotubes when cocultured with muscle cells in vivo. The abilities to expand ex vivo, genetically manipulate, and cryogenically store umbilical cord blood HSC in addition to their potential to contribute to repair of other tissues holds great promise for future stem cell–based therapies.

Although umbilical cord blood is known to be a rich source of HSC *(44, 45)*, the existence of MSC in umbilical cord blood has been somewhat controversial *(46)*. However, in recent studies, MSC has been isolated from cord blood through methods used for isolation of MSC from bone marrow *(47)*. The umbilical cord–derived MSC displayed a fibroblast-like morphology and were smooth muscle actin and fibronectin positive. This suggests that they may be related to the cells isolated from umbilical cord matrix, which may migrate into the cord blood circulation. Other groups have isolated MSC from umbilical cord blood that could be expanded in culture and induced to differentiate into osteocytes, chondrocytes, and adipocytes as well as hepatocytes of mesenchymal origin *(48)*. They were also able to induce the cells to express markers for neurons and glia Hou et al. isolated MSC from umbilical cord blood by negative selection. These cells do not express CD34, CD11a, or CD11b, but do express CD29 and CD71, which is identical to MSC derived from bone marrow *(49)*. Hou et al. also isolated clonal populations of MSC that could differentiate into adipocytes, chondrocytes, osteocytes, hepatocytes, neuronal, and glial cells based on expression of specific markers.

Cells that resemble neural stem cells have been isolated from umbilical cord blood *(50)*. Nestin, an intermediate filament expressed in neural precursors, is expressed by a large percentage of human cord blood monocytes that also coexpress CD133. However, nestin expression was not detected in adult monocytes *(50)*. Buzanska et al. *(51)* showed that nestin-expressing cells from umbilical cord blood could be directed to differentiate into early neurons that expressed TUJ1 (a neuron-specific class III β-tubulin), astrocytes expressing GFAP, and galactocerebrosidase expressing oligodendrocytes by treatment with brain-derived neurotrophic factor and retinoic acid. Similarly, other studies have shown that CD45-negative cells from umbilical cord blood could be expanded in culture and then be induced to form cells that express neuronal and glial markers TUJ1 and GFAP *(52)*. Many other studies have shown the potential for cells from cord blood to differentiate into cells that express neuronal or glial proteins using a number of different induction protocols *(53)*. Interestingly, many of the proteins are expressed in umbilical cord cells without any treatment to induce them. For example, GFAP was expressed in about one-third of the isolated cells. This was increased by treatment with retinoic acid. Similar results

were found for expression of NeuN. These studies show that a population of cells within umbilical cord blood express markers and have properties very similar to those of umbilical cord matrix cells and neural precursor cells (*see* Table 1).

3.3. Other Extraembryonic Stem Cells

Other cells with stem cell–like properties have been identified in the extraembryonic tissues. Oct-4–expressing cells have been identified in human amniotic fluid *(29)*. Amniotic fluid cells express stem cell factor, smooth muscle actin, and vimentin and are rapidly proliferating compared with adult cells *(54)*. They may also express telomerase as telomerase activity has been detected in amniotic fluid *(55)*. Amniotic cells also express a number of glial and neuronal proteins, including neurofilament proteins, microtubule-associated protein 2, GFAP, ,2',3'-cyclic nucleotide 3'-phosphodiesterase, myelin basic protein, and galactocerebroside *(56, 57)*. These properties are similar to those of cells isolated from umbilical cord matrix, suggesting that they may have a common origin.

An interesting observation made by several investigators is that many neuronal and glial proteins are expressed in extraembryonic tissues. Initially, expression of some neuronal and glial proteins, NSE and S100, in cord blood and amniotic fluid was thought to be indicative of neonatal neuronal damage *(58–61)*. But recent studies have shown that high levels of NSE and S-100 are expressed in umbilical cord blood after normal delivery. They are expressed at higher levels in the artery than venous blood, suggesting fetal origin *(62)*. Wijnberger et al. did a more extensive analysis of neuronal and glial protein expression in the placenta and umbilical cord, looking for expression of S-100, NSE, GFAP, and GAP43 *(63)*. They found that many cell types, including myofibroblasts of Wharton's jelly, are positive for NSE and S-100, as are cells of the vascular wall, amnion epithelium, and macrophages and monocytes in umbilical cord blood. GFAP and GAP43 were not detected, however. S-100 is also expressed in placental tissues *(64)*. These results suggest that extraembryonic tissues are possibly a rich source of stem cells with neural precursor type properties.

4. RELATIONSHIP TO ES, EG, AND ADULT STEM CELLS

ES cells are derived from the inner cell mass of the blastula. EG cells are derived proximal to the epiblast, residing temporarily in a protected environment of the yolk stalk so that they remain undifferentiated. Adult stem cells are found in most tissues, as well as in circulation. Adult stem cells are usually quiescent but become activated under conditions of stress or injury. What are the origins of adult stem cells and how do they keep from differentiating? These are some of the most critical questions in stem cell biology. It has been suggested that stem

cells may not be the first cells to show up in a tissue, but rather may appear later in development when they can populate adult niches. Adult stem cells may be differentiated appropriately for their tissue, but also have other potentials if in a different microenvironment.

Are multipotential adult stem cells related to the primitive stem cells of the umbilical cord? Most multipotential adult stem cells share common characteristics with the myofibroblast-like cells isolated from umbilical cord matrix *(31)*. Postnatal stem cells in the adult, from a wide variety of sources, appear to be capable of differentiation into multiple tissue types. Cells derived from bone marrow *(65)*, skin *(66)*, astrocytes *(67)*, synoviocytes *(68)*, adipose *(69)*, and dental pulp *(70)* have recently been shown to be multipotential. Many of these multipotential stem cells may have a common precursor in that they are tissue-specific myofibroblasts. Myofibroblasts are found throughout the body and include bone marrow stromal cells, astrocytes, synoviocytes, and pericytes *(71)*. Myofibroblasts in the adult take part in growth, development, and repair of normal tissue. They can also be the cause of organ fibrosis, scar formation, and tumors. Myofibroblasts have some tissue-specific functions but are similar in morphology, function, and biochemistry regardless of their location *(71)*. Perhaps myofibroblasts or their precursors exist as a pool of pluripotent stem cells that exist in equilibrium between stem cells that are buried in the diverse organs and those that circulate from the bone marrow, similar to monocytes and macrophages as suggested by Labat for adult stem cells *(72)*. There are intrinsic differences in fetal versus adult myofibroblasts that regulate their responses to cytokines, which in turn may account for the ability for scarless repair by fetal myofibroblasts *(73)*. This may be a critical characteristic that favors younger myofibroblasts, such as those isolated from umbilical cord matrix for therapeutic applications.

5. UMBILICAL CORD STEM CELLS AND THE IMMUNE SYSTEM

Although much of the enthusiasm about the potentials for therapeutic applications of ES cells is based on the hope that they will evade the immune system, very little work has been done to investigate this potential. Immunologic rejection may be an important barrier for ES cell–based therapies if MHC molecules responsible for immune-mediated graft rejection are expressed by ES cells after they differentiate. Human ES cells express HLA class I but not class II molecules. Expression of both classes of molecules increases with differentiation in vitro or in vivo *(74)*. As with ES cells, mesenchymal stem cells express low levels of HLA class I molecules but not class II *(75)*. Importantly, they were able to

Job: Lester (307-2)
Chapter: 03/Mitchell
Pub Date:
Template: CE/6x9/Template/Rev.08.03
Operator: SV
Date: 9/04
Revision: 1st Pass

suppress mixed lymphocytic cultures and retained this capability even after differentiation.

Tumor formation (teratomas) by ES cells is a major hurdle that needs to be overcome before this source of cells can be used in therapeutic applications. Preliminary findings show that, unlike ES cells, human umbilical cord matrix cells do not form tumors in immune compromised mice *(23)*. Porcine umbilical cord matrix cells do not illicit an immune response when injected into rat brain or muscle, nor are they rejected at 4 weeks *(24)*. The mechanism of this immune evasion is not known but may involve the low expression of HLA class I molecules and expression of HLA-G *(23)*, a nonclassical HLA that suppresses immune response at the maternal-fetal interface *(76)* and in muscle *(77)*.

Umbilical cord blood HSC have low immunogenicity with a lower incidence of graft-versus-host disease when used for transplantation in cancer patients, even when the number of HLA markers that are matched are lower *(78)*. The mechanism of this potential to evade the immune system is not understood. However, β2-microglobulin is expressed constitutively in cord blood cells *(79)* and is known to be an integral part of MHC expression in killer T cells and, thus, may play a role in immune evasion of umbilical cord blood HSC *(80)*. Stem cells from umbilical cord appear to have the unique ability to evade the immune system, which makes their use therapeutically particularly exciting. More research on the mechanisms by which umbilical cord stem cells suppress immune response and how long after differentiation this is maintained is essential.

6. POTENTIAL FOR CELL-BASED THERAPIES

Umbilical cord blood is commonly used in cell-based therapies today for reconstitution of the bone marrow after radiation for cancers of the blood *(36)*. There are some new experimental therapies using bone marrow transplant with cord blood cells being developed for other diseases. Umbilical cord blood transplantation in Wiskott Aldrich syndrome, which results in severe immune deficiency and early death if not treated, was found to result in rapid and reliable recovery of immune function, with low risk of graft-versus-host disease *(81)*. Using umbilical cord blood stem cells taken from unrelated donors, Staba et al. *(82)* treated children with Hurler's syndrome, who lack of a functional enzyme, alpha-L-iduronidase. These researchers were able to treat these patients without radiation and to have improvement in survival and less neuronal degeneration than Hurler's patients who received bone marrow transplants. The researchers speculate that stem cells from cord blood may transport α-L-iduronidase across the blood–brain barrier more effectively. In addition, they are younger cells and do not have to be matched as closely. Research is under way to expand the use of umbilical cord blood cells to treat other disorders such as β-thalassemia *(83)*.

Job: Lester (487-2)
Chapter: 03/Mitchell
Pub Date:
Template: CE/6x9/Template/Rev.04.03
Operator: SV
Date: 9/04
Revision: 1st Pass

Animal models suggest that umbilical cord blood cells may be useful in treatment of amyotrophic lateral sclerosis by slowing motor neuron degeneration when injected intravenously *(84)*. Ende and coworkers found that intravenous injection of umbilical cord blood cells could extend the survival of several mouse knockout models of human disease, including amyotrophic lateral sclerosis *(85)*, Alzheimer's *(85)*, Huntington's *(86)*, Parkinson's *(87)*, and type 1 diabetes *(88)*. Human umbilical cord blood cells also improve the mobility of rats with spinal cord injuries when injected intravenously. Cord blood cells were observed in the areas of injury of spinal cord but not others and never seen in the control, uninjured animals *(89)*. Similarly, umbilical cord blood cells were able to improve function in a stroke model in the rat when injected intravenously. The human umbilical cord blood cells differentiated into cells that expressed glial or neuronal markers *(90)*. This suggests that umbilical cord blood cells have the ability to target to and heal neurologic defects.

Cells from umbilical cord matrix may also be a source of cells for treatment of neurodegenerative disease. Medicate et al. *(91)* treated rats with a unilateral 6-hydroxydopamine (6-OHDA) lesion that caused parkinsonian-like symptoms. Four weeks after the 6-OHDA lesion, rats were injected with umbilical cord matrix cells or sham transplants. Four weeks after transplantation, there was a significant decrease in apomorphine-induced rotatory behavior in the parkinsonian rats, which received umbilical cord matrix cell transplants, as compared with parkinsonian rats that received a sham transplant. Normal rats, without 6-OHDA lesions, were transplanted with umbilical cord matrix cells but showed no changes in behavior. This work suggests that umbilical cord matrix cells can target areas of neurodegeneration and play a role in healing of neural tissue. Amniotic cells may have a similar potential *(92)*. Labeled amniotic epithelial cells were injected into monkeys with spinal cord injuries. Some labeled neurons were subsequently found in the spinal cord. Glial scar formation was decreased compared with animals that did not receive amniotic epithelial cells. More importantly, the function of the animals improved suggesting that amniotic epithelial cells help in axon regrowth. These studies suggest that cells from umbilical cord blood and other cells from extraembryonic tissues may be an important source of stem cells for a variety of therapeutic applications.

7. SUMMARY

There is much hope today for the many potential benefits that can be achieved through stem cell research, including a better understanding of the basic biology of stem cells that may provide insights into cancer when proper control of proliferation and differentiation have gone awry, for developmental processes, and for drug discovery. There is significant potential to discover new drugs through

stem cell research that will increase the proliferative capacity of specific populations of cells in the brain to ameliorate Parkinson's disease or in the islets to produce new insulin-producing cells or discover new chemotherapeutic agents that target the cancer stem cell and thus improve long-term survival of cancer patients. What is clear is that there is much yet to be learned; stem cell biology and regenerative medicine are in their infancy. We need to study cells from many sources to be able to harness these potentials. The cells from the umbilical cord and other extraembryonic tissues are a particularly exciting and promising source of primitive stem cells based on their ready availability, low immunogenicity, and lack of tumorigenicity. The study of extraembryonic stem cells may also reveal the origins of the adult stem cell. Extraembryonic stem cells may also be a particularly useful tool in drug development because of their ready availability, making it possible to harvest cells that represent a genetically diverse population or stem cells that carry specific genetic defects.

ACKNOWLEDGMENTS

Supported by P20 RR 15563-02 COBRE-NIH and RO1-NS/HL36124. Jeremy Traas is also acknowledged for his research contributions.

REFERENCES

1. McKay R. Stem cells in the central nervous system. Science 1997;276:66–71.
2. Gordon MY, Blackett NM. Reconstruction of the hematopoietic system after stem cell transplantation. Cell Transplant 1998;7:339–344.
3. Scheffler B, Horn M, Blumcke I, et al. Marrow-mindedness: a perspective on neuropoiesis. Trends Neurosci 1999;22:348–357.
4. Smith A. Embryo-derived stem cells: of mice and men. Annu Rev Cell Dev Biol 2001;17:435–462.
5. Hubner K, Fuhrmann G, Christenson LK, et al. Derivation of oocytes from mouse embryonic stem cells. Science 2003;300:1251–1256.
6. Toyooka Y, Tsunekawa N, Akasu R, Noce T. Embryonic stem cells can form germ cells in vitro. PNAS 2003;100:11457–11462.
7. Clark AT, Bodnar MS, Fox M, et al. Spontaneous differentiation of germ cells from human embryonic stem cells in vitro. Hum Mol Genet 2004;13:727–739.
8. Shamblott MJ, Axelman J, Wang S, et al. Derivation of pluripotent stem cells from cultured human primordial germ cells. PNAS 1998;95:13726–13731.
9. Paul G, Li JY, Brundin P. Stem cells: hype or hope? Drug Discov Today 2002;7:295–302.
10. Nanaev AK, Kohnen G, Milovanov AP, Domogatsky SP, Kaufmann P. Stromal differentiation and architecture of the human umbilical cord. Placenta 1997;18:53–64.
11. Takechi K, Kuwabara Y, Mizuno M. Ultrastructural and immunohistochemical studies of Wharton's jelly umbilical cord cells. Placenta 1993;14:235–245.
12. Gardner RL. Cell lineage and cell commitment in the early mammalian embryo. Mead Johnson Symp Perinat Dev Med 1979;XX:18–24.

Au: ref 12 - Please provide volume number.

13. Lawson KA, Meneses JJ, Pedersen RA. Clonal analysis of epiblast fate during germ layer formation in the mouse embryo. Development 1991;113:891–911.

14. Vogler H. Human Blastogenesis. Formation of the Extraembryonic Cavities. Bibliotheca Anatomica 30. Karger, Basel, 1987.
15. Moore MA, Metcalf D. Ontogeny of the haemopoietic system: yolk sac origin of in vivo and in vitro colony forming cells in the developing mouse embryo. Br J Haematol 1970;18:279–296.
16. Weissman IL, Warnke R, Butcher EC, Rouse R, Levy R. The lymphoid system. Its normal architecture and the potential for understanding the system through the study of lymphoproliferative diseases. Hum Pathol 1978;9:25–45.
17. Mintz B, Russell ES. Gene-induced embryological modifications of primordial germ cells in the mouse. J Exp Zool 1957;134:207–237.
18. Tre, LL, Rosselot C, Kierszenbaum AL. Primordial germ cells: what does it take to be alive? Mol Reprod Dev 2004;68:1–4.
19. Schneider DT, Schuster AE, Fritsch MK, et al. Multipoint imprinting analysis indicates a common precursor cell for gonadal and nongonadal pediatric germ cell tumors. Cancer Res 2001;61:7268–7276.
20. End, M. History of umbilical cord blood transplantation. Lancet 1995;346:1161.
21. Ende N. Berashis cells in human umbilical cord blood vs. embryonic stem cells. J Med 2002;33:167–171.
22. von Drygalski A, Adamson J. Placental/umbilical cord blood (PCB) stem cells for transplantation: early clinical outcomes and the status of ex vivo expansion strategies. Keio J Med 2000;49:141–151.
23. Truas J, Kaptur R, Schermerhorn T, Chun R, Mitchell KE Stem cell gene array analysis of Oct-4 positive human umbilical cord matrix cells. Mol Cell Biol 2003;14:115a.
24. Weiss ML, Mitchell KE, Hix JE, et al. Transplantation of porcine umbilical cord matrix cells into the rat brain. Exp Neurol 2003;182:288–299.
25. Suzuki N, Rohdewohld H, Neuman T, Gruss P, Scholer HR. Oct-6: a POU transcription factor expressed in embryonal stem cells and in the developing brain. EMBO J 1990;9:3723–3732.
26. Pesce M, Scholer HR. Oct-4: control of totipotency and germline determination. Mol Reprod Dev 2000;55:452–457.
27. Niwa H, Miyazaki J, Smith AG. Quantitative expression of Oct-3/4 defines differentiation, dedifferentiation or self-renewal of ES cells. Nat Genet 2000;24:372–376.
28. Pochampally RR, Smith JR, Ylostalo J, Prockop DJ. Serum deprivation of human marrow stromal cells (hMSCs) selects for a subpopulation of early progenitor cells with enhanced expression of OCT-4 and other embryonic genes. Blood 2004;103:1647–1652.
29. Prusa AR, Marton E, Rosner M, Bernaschek G, Hengstschlager M. Oct-4-expressing cells in human amniotic fluid: a new source for stem cell research? Hum Reprod 2003;18:1489–1493.
30. Shamblott MJ, Axelman J, Littlefield JW, et al. Human embryonic germ cell derivatives express a broad range of developmentally distinct markers and proliferate extensively in vitro. Proc Natl Acad Sci USA 2001;98:113–118.
31. Mitchell KE, Weiss ML, Mitchell BM, et al. Matrix cells from Wharton's jelly form neurons and glia. Stem Cells 2003;21:50–60.
32. Helwig B, Van Wye T, Hoynowski S, Mitchell KE. Defining key proteins in stem cell based neuronal development using proteomics. Mol Cell Biol 2003;14:115a.
33. Woodbury D, Schwarz EJ, Prockop DJ, Black IB. Adult rat and human bone marrow stromal cells differentiate into neurons. J Neurosci Res 2000;61:364–370.
34. Broxmeyer HE, Douglas GW, Hangoc G, et al. Human umbilical cord blood as a potential source of transplantable hematopoietic stem/progenitor cells. Proc Natl Acad Sci USA 1989;86:3828–3832.
35. Sirchia G, Rebulla P. Placental/umbilical cord blood transplantation. Haematologica 1999;84:738–747.

36. Gluckman E, Rocha V, Boyer-Chammard A, et al. Outcome of cord-blood transplantation from related and unrelated donors. Eurocord Transplant Group and the European Blood and Marrow Transplantation Group. N Engl J Med 1997;337:373–381.
37. Murohara T, Ikeda H, Duan J, et al. Transplanted cord blood-derived endothelial precursor cells augment postnatal neovascularization. J Clin Invest 2000;105:1527–1536.
38. Wu AG, Michejda M, Mazumder A, et al. Analysis and characterization of hematopoietic progenitor cells from fetal bone marrow, adult bone marrow, peripheral blood, and cord blood. Pediatr Res 1999;46:163–169.
39. Mayani H, Lansdorp PM. Biology of human umbilical cord blood-derived hematopoietic stem/progenitor cells. Stem Cells 1998;16:153–165.
40. Lansdorp PM, Poon S, Chavez E, et al. Telomeres in the haemopoietic system. Ciba Found Symp 1997;211:209–218; discussion 219–222.
41. Globerson A. Hematopoietic stem cells and aging. Exp Gerontol 1999;34:137–146.
42. Kashiwakura I, Takahashi TA. Basic fibroblast growth factor-stimulated ex vivo expansion of haematopoietic progenitor cells from human placental and umbilical cord blood. Br J Haematol 2003;122:479–488.
43. Pesce M, Orlandi A, Iachininoto MG, et al. Myoendothelial differentiation of human umbilical cord blood-derived stem cells in ischemic limb tissues. Circ Res 2003;93:e51–e62.
44. Hows JM. Status of umbilical cord blood transplantation in the year 2001. J Clin Pathol 2001;54:428–434.
45. Benito AI, Diaz MA, Gonzalez-Vicent M, Sevilla J, Madero L. Hematopoietic stem cell transplantation using umbilical cord blood progenitors: review of current clinical results. Bone Marrow Transplant 2004;33:675–690.
46. Mareschi K, Biasin E, Piacibello W, Aglietta M, Madon E, Fagioli F. Isolation of human mesenchymal stem cells: bone marrow versus umbilical cord blood. Haematologica 2001;86:1099–1100.
47. Romanov YA, Svintsitskaya VA, Smirnov VN. Searching for alternative sources of postnatal human mesenchymal stem cells: candidate MSC-like cells from umbilical cord. 2003;Stem Cells 21:105–110.
48. Lee OK, Kuo TK, Chen WM, Lee KD, Hsieh SL, Chen TH. Isolation of multipotent mesenchymal stem cells from umbilical cord blood. Blood 2004;103:1669–1675.
49. Hou L, Cao H, Wang D, et al. Induction of umbilical cord blood mesenchymal stem cells into neuron-like cells in vitro. Int J Hematol 2003;78:256–261.
50. Ha Y, Lee JE, Kim KN, Cho YE, Yoon DH. Intermediate filament nestin expressions in human cord blood monocytes (HCMNCs). Acta Neurochir (Wien) 2003;145:483–487.
51. Buzanska L, Machaj EK, Zablocka B, Pojda Z, Domanska-Janik K. Human cord blood-derived cells attain neuronal and glial features in vitro. J Cell Sci 2002;115:2131–2138.
52. Bicknese AR, Goodwin HS, Quinn CO, Henderson VC, Chien SN, Wall DA. Human umbilical cord blood cells can be induced to express markers for neurons and glia. Cell Transplant 2002;11:261–264.
53. Sanchez-Ramos JR, Song S, Kamath SG, et al. Expression of neural markers in human umbilical cord blood. Exp Neurol 2001;171:109–115.
54. Kaviani A, Perry TE, Dzakovic A, Jennings RW, Ziegler MM, Fauza DO. The amniotic fluid as a source of cells for fetal tissue engineering. J Pediatr Surg 2001;36:1662–1665.
55. Mosquera A, Fernandez JL, Campos A, Goyanes VJ, Ramiro-Diaz J, Gosalvez J. Simultaneous decrease of telomere length and telomerase activity with ageing of human amniotic fluid cells. J Med Genet 1999;36:494–496.
56. Sakuragawa N, Thangavel R, Mizuguchi M, Hirasawa M, Kamo I. Expression of markers for both neuronal and glial cells in human amniotic epithelial cells. Neurosci Lett 1996;209:9–12.

Job: Lester (487-2)
Chapter: 03/Mitchell
Pub Date:
Template: CE/6x9/Template/Rev.04.03

Operator: SV
Date: 9/04
Revision: 1st Pass

57. Uchida S, Inanaga Y, Kobayashi M, Hurukawa S, Araie M, Sakuragawa N. Neurotrophic function of conditioned medium from human amniotic epithelial cells. J Neurosci Res 2000;62:585–590.
58. Zinsmeyer J, Marangos PJ, Issel EP, Gross J. Neuron specific enolase in amniotic fluid—a possible indicator for fetal distress and brain implication. J Perinat Med 1987;15:199–202.
59. Elimian A, Figueroa R, Verma U, Visintainer P, Sehgal PB, Tejani N. Amniotic fluid neuron-specific enolase: a role in predicting neonatal neurologic injury? Obstet Gynecol 1998;92:546–550.
60. Kintzel K, Sonntag J, Strauss E, Obladen M. Neuron-specific enolase: reference values in cord blood. Clin Chem Lab Med 1998;36:245–247.
61. Gazzolo D, Vinesi P, Marinoni E, et al. S100B protein concentrations in cord blood: correlations with gestational age in term and preterm deliveries. Clin Chem 2000;46:998–1000.
62. Amer-Wahlin I, Herbst A, Lindoff C, Thorngren-Jerneck K, Marsal K, Alling C. Brain-specific NSE and S-100 proteins in umbilical blood after normal delivery. Clin Chim Acta 2001;304:57–63.
63. Wijnberger LD, Nikkels PG, van Dongen AJ, et al. Expression in the placenta of neuronal markers for perinatal brain damage. Pediatr Res 2002;51:492–496.
64. Marinoni E, Di Iorio R, Gazzolo D, et al. Ontogenetic localization and distribution of S-100beta protein in human placental tissues. Obstet Gynecol 2002;99:1093–1099.
65. Jiang Y, Jahagirdar BN, Reinhardt RL, et al. Pluripotency of mesenchymal stem cells derived from adult marrow. Nature 2002;418:41–49.
66. Toma JG, Akhavan M, Fernandes KJ, et al. Isolation of multipotent adult stem cells from the dermis of mammalian skin. Nat Cell Biol 2001;3:778–784.
67. Laywell ED, Rakic P, Kukekov VG, Holland EC, Steindler DA. Identification of a multipotent astrocytic stem cell in the immature and adult mouse brain. Proc Natl Acad Sci USA 2000;97:13883–13888.
68. De Bari C, Dell'Accio F, Tylzanowski P, Luyten FP. Multipotent mesenchymal stem cells from adult human synovial membrane. Arthritis Rheum 2001;44:1928–1942.
69. Zuk PA, Zhu M, Ashjian P, et al. Human adipose tissue is a source of multipotent stem cells. Mol Biol Cell 2002;13:4279–4295.
70. Miura M, Gronthos S, Zhao M, et al. SHED: stem cells from human exfoliated deciduous teeth. Proc Natl Acad Sci USA 2003;100:5807–5812.
71. Powell, DW, Mifflin RC, Valentich JD, Crowe SE, Saada JI, West AB. Myofibroblasts. I. Paracrine cells important in health and disease. Am J Physiol 1999;277:C1–C9.
72. Labat ML. Stem cells and the promise of eternal youth: embryonic versus adult stem cells. Biomed Pharmacother 2001;55:179–185.
73. Moulin V, Tam BY, Castilloux G, et al. Fetal and adult human skin fibroblasts display intrinsic differences in contractile capacity. J Cell Physiol 2001;188:211–222.
74. Bradley JA, Bolton EM, Pedersen RA. Stem cell medicine encounters the immune system. Nat Rev Immunol 2002;2:859–871.
75. Le Blanc K, Tammik C, Rosendahl K, Zetterberg E, Ringden O. HLA expression and immunologic properties of differentiated and undifferentiated mesenchymal stem cells. Exp Hematol 2003;31:890–896.
76. Rouas-Freiss N, Kirszenbaum M, Dausset J, Carosella ED. Fetomaternal tolerance: role of HLA-G molecule in the protection of the fetus against maternal natural killer activity). C R Acad Sci III 1997;320:385–392.
77. Wiendl H, Mitsdoerffer M, Hofmeister V, et al. The non-classical MHC molecule HLA-G protects human muscle cells from immune-mediated lysis: implications for myoblast transplantation and gene therapy. Brain 2003;126:176–185.

Uncorrected Proof Copy

Job: Lester (407-2)
Chapter: 03/Mitchell
Pub Date:
Template: CE/6x9/Template/Rev.04/03

Operator: SV
Date: 3/04
Revision: 1st Pass

78. Barker JN, Wagner JE. Umbilical cord blood transplantation: current practice and future innovations. Crit Rev Oncol Hematol 2003;48:35–43.
79. Beerheide W, von Mach MA, Ringel M, et al. Downregulation of beta2-microglobulin in human cord blood somatic stem cells after transplantation into livers of SCID-mice: an escape mechanism of stem cells? Biochem Biophys Res Commun 2002;294:1052–1063.
80. Hoglund P, Glas R, Menard C, et al. Beta2-microglobulin-deficient NK cells show increased sensitivity to MHC class I-mediated inhibition, but self tolerance does not depend upon target cell expression of H-2Kb and Db heavy chains. Eur J Immunol 1998;28:370–378.
81. Knutsen AP, Steffen M, Wassmer K, Wall DA. Umbilical cord blood transplantation in Wiskott Aldrich syndrome. J Pediatr 2003;142:519–523.
82. Staba SL, Escolar ML, Poe M, et al. Cord-blood transplants from unrelated donors in patients with Hurler's syndrome. N Engl J Med 2004;350:1960–1969.
83. Hall JG, Martin PL, Wood S, Kurtzberg J. Unrelated umbilical cord blood transplantation for an infant with beta-thalassemia major. J Pediatr Hematol Oncol 2004;26:382–385.
84. Garbuzova-Davis S, Willing AE, Zigova T, et al. Intravenous administration of human umbilical cord blood cells in a mouse model of amyotrophic lateral sclerosis: distribution, migration, and differentiation. J Hematother Stem Cell Res 2003;12:255–270.
85. Ende N, Weinstein F, Chen R, Ende M. Human umbilical cord blood effect on sod mice (amyotrophic lateral sclerosis). Life Sci 2000;67:53–59.
86. End, N, Chen R. Human umbilical cord blood cells ameliorate Huntington's disease in transgenic mice. J Med 2001;32:231–240.
87. Ende N, Chen R. Parkinson's disease mice and human umbilical cord blood. J Med 2002;33:173–180.
88. Ende N, Chen R, Mack R. NOD/LtJ type I diabetes in mice and the effect of stem cells (Berashis) derived from human umbilical cord blood. J Med 2002;33:181–187.
89. Saporta S, Kim JJ, Willing AE, Fu ES, Davis CD, Sanberg PR. Human umbilical cord blood stem cells infusion in spinal cord injury: engraftment and beneficial influence on behavior. J Hematother Stem Cell Res 2003;12:271–278.
90. Chen J, Sanberg PR, Li Y, et al. Intravenous administration of human umbilical cord blood reduces behavioral deficits after stroke in rats. Stroke 2001;32:2682–2688.
91. Medicetty S, Bledsoe AR, Mitchell KE, Troyer D, Weiss ML. Transplantation of human umbilical cord matrix stem cells alleviates apomorphine-induced rotations in Parkinsonian rats. Neuroscience Meeting Abstract, 2003.
92. Sankar V, Muthusamy R. Role of human amniotic epithelial cell transplantation in spinal cord injury repair research. Neuroscience 2003;118:11–17.